

Alteration of claudins by C-CPE affects lung expansion in cultured mouse and chick embryonic lung

Simon La Charité-Harbec

Department of Human Genetics
McGill University, Montréal, Québec, Canada
June 2019

A thesis submitted to the Faculty of Graduate and Postdoctoral Studies in partial fulfillment of the requirements of the degree of Master of Science

© Simon La Charité-Harbec, 2019

Abstract

The claudins are a family of integral membrane proteins located in tight junctions. Tight junctions are protein complexes that link the membrane of adjacent epithelial cells together. Claudins regulate paracellular transport between cells in mature epithelia. Interestingly, claudins are expressed in several branching organs during development, for example, the kidneys and the lungs, even prior to the initiation of paracellular transport. Previous results from my laboratory showed that the removal of a subset of claudins using the non-toxic protein reagent C-CPE (a truncated form of *Clostridium perfringens* enterotoxin) resulted in the reduction of branching in mouse embryonic kidney explants.

To determine if claudins are required for lung branching morphogenesis, I examined their role during early lung development. Using *in situ* hybridization and immunofluorescence, I showed that Cldn1, -3 and -10 mRNA and protein are expressed in the epithelial cells of chick lungs during the first stages of branching morphogenesis. When I cultured embryonic chick and mouse lung explants in the presence of C-CPE, no difference in lung bud count was observed. However, a significant decrease in the lumen perimeter and the lumen area was detected in the chick lung explants after 48h of culture ($P = 0.05$). Mouse lung explants exhibited a similar phenotype, but further experiments are needed to confirm if claudins are important for lumen expansion in the developing mouse lung. Immunofluorescence of the C-CPE-sensitive Cldn3 was performed on chick lung cryosections to determine if the phenotype was due to the removal of those C-CPE-sensitive claudins. Cldn3 appeared to colocalize less with ZO-1, a tight junction marker, in C-CPE-treated explants. Accumulation of Cldn3 in the lumen was also observed in some C-CPE-treated explants. Further replicates are needed to confirm the effect of C-CPE on sensitive claudins. Cldn3 immunofluorescence was also performed on whole mount mouse explants and abnormal expression was observed at the basolateral side of the epithelial cells. These data suggest that the effects on lumen area in the C-CPE-treated lungs could be due to a depletion in C-CPE-sensitive claudins at the apical cell surface. In conclusion, the data in this thesis shows that C-CPE-sensitive claudins do not exhibit a direct role in chick or mouse lung branching morphogenesis, but rather that these claudins may play a role in the regulation of luminal fluid accumulation.

Résumé

Les claudines sont une famille de protéines membranaires intégrales qui se trouvent dans les jonctions serrées. Les jonctions serrées sont des complexes protéiques reliant la membrane de cellules épithéliales adjacentes. Les claudines régulent le transport dans l'espace paracellulaire dans les couches de cellules épithéliales matures. Il est intéressant de constater que les claudines sont exprimées dans plusieurs organes ramifiés, comme le rein et les poumons, au cours de leur développement, et ce même avant le début du transport paracellulaire. Des résultats antérieurs de mon laboratoire ont montré que le retrait d'un sous-ensemble de claudines à l'aide de la protéine non toxique C-CPE (une forme tronquée de l'entérotoxine de la bactérie *Clostridium perfringens*) entraînait une réduction de la ramification dans des explants de reins embryonnaires de souris.

Pour déterminer si les claudines sont nécessaires à la morphogenèse de ramification des poumons, j'ai examiné leur rôle dans des explants de poumons embryonnaires de poulet et de souris. En utilisant l'hybridation *in situ* et l'immunofluorescence, j'ai montré que l'ARNm et la protéine des Cldn1, -3 et -10 sont exprimés dans les cellules épithéliales des poumons d'embryons de poulet au cours des premiers stades de la morphogenèse de ramification. Lorsque j'ai mis en culture des explants pulmonaires d'embryons de poulet et de souris avec du C-CPE, aucune différence dans le nombre de bourgeons pulmonaires n'a été observée. Cependant, une diminution significative du périmètre de la lumière et de la surface de la lumière a été détectée dans les explants de poumon de poussin après 48 heures de culture ($P = 0,05$). Les explants de poumon de souris présentaient un phénotype similaire, mais des mesures supplémentaires sont nécessaires pour confirmer le rôle des claudines dans l'expansion de la lumière pulmonaire. Une immunofluorescence marquant la Cldn3, qui est sensible au C-CPE, a été réalisée sur des cryosections de poumon d'embryons de poulet afin de déterminer si le phénotype était dû au retrait des claudines par le C-CPE. La Cldn3 semble moins se colocaliser avec ZO-1, un marqueur de jonction serrée, dans les explants traités avec du C-CPE. Une accumulation de Cldn3 dans la lumière a également été observée dans certains explants traités avec du C-CPE. D'autres réplicats sont nécessaires pour confirmer l'effet du C-CPE sur les claudines sensibles au C-CPE. Une immunofluorescence marquant la Cldn3 a également été réalisée sur des explants de souris complets et une expression anormale a été observée sur le côté basolatéral des cellules épithéliales. Ces données suggèrent que le phénotype de réduction de la surface de la lumière dans les poumons cultivés avec du C-CPE pourrait être dû à une réduction de la localisation des

claudines sensibles au C-CPE sur la surface apicale des cellules épithéliales. En conclusion, les données de ce projet démontrent que les claudines sensibles au C-CPE ne jouent pas un rôle direct dans la morphogenèse de ramification des poumons chez le poussin ou la souris, mais ces claudines pourraient jouer un rôle dans la régulation de l'accumulation de liquide luminal.

Table of contents

Abstract	2
Résumé	3
Table of contents	5
List of figures	7
List of tables.....	8
List of abbreviations	9
Acknowledgements	11
Format of the thesis	13
Contribution of authors.....	14
CHAPTER 1: Introduction.....	15
1.1 Tight junctions	15
1.1.1 Tight junction proteins	18
1.1.1.1 Claudins	18
1.1.1.2 Occludin.....	21
1.1.1.3 Junction adhesion molecules	22
1.1.1.4 Zonula occludens family of tight junction proteins.....	22
1.2 <i>Clostridium perfringens</i> enterotoxin	23
1.3 Claudins during development	25
1.3.1 Mouse claudin knock-out and knockdown assays	25
1.4 Branching morphogenesis.....	28
1.5 Lung development.....	29
1.5.1 Claudins during lung development.....	31
1.6 Hypothesis and objectives.....	32
1.6.1 Hypothesis	32
1.6.2 Objectives:	32
CHAPTER 2: Materials and methods	33
2.1 Embryonic lung collection	33
2.2 Whole mount <i>in situ</i> hybridization	33
2.3 Paraffin sections	35
2.4 Cryosections	36
2.5 Immunofluorescence on cryosections	36
2.6 GST-C-CPE and GST protein production	37

2.7 Chick and mouse embryonic lung explants culture.....	40
2.8 Chick lung measurements	40
2.9 Statistical analyses.....	41
2.10 Whole mount immunofluorescence	41
CHAPTER 3: Results	42
3.1 Analysis of claudin expression during chick lung branching morphogenesis.....	42
3.1.1 Claudin mRNA expression	42
3.1.2 Claudin protein expression.....	45
3.2 Establishing conditions to grow embryonic chick lungs <i>ex vivo</i>	51
3.3 Treatment with C-CPE decreases the lumen area and the lumen perimeter in embryonic chick lung.....	57
3.4 C-CPE localizes to the apical side of the epithelial cells in treated lungs.....	58
3.5 α SMA immunofluorescence on C-CPE treated chick lung explants was not different than controls.....	58
3.6 Preliminary results of molecular analysis show partial removal of Claudin-3 in C-CPE treated chick lungs.	61
3.7 Treatment with C-CPE seems to decrease lumen area in embryonic mouse lung explants.	61
3.8 Molecular analysis shows disrupted Claudin-3 localization in GST-C-CPE treated mouse lungs.	63
CHAPTER 4: Discussion	65
4.1 Characterization of claudin expression in chick lung at the formation of secondary bronchi.	65
4.2 C-CPE-treated lung explants have reduction in lumen area.	67
CHAPTER 5: Conclusions and future directions.....	72
CHAPTER 6: References	74

List of figures

Figure 1. Schematic of the different functions of tight junctions.	16
Figure 2. Schematic of tight junction protein complex.	17
Figure 3. Schematic of claudin protein.	19
Figure 4. Schematic of the early steps in lung branching morphogenesis.	29
Figure 5. Analysis of <i>Claudin</i> expression in E4-E6 chick lungs.	45
Figure 6. Characterization of Claudin-1 and -3 expression in branching chick lungs.	47
Figure 7. Characterization of Claudin-4 and-5 expression in branching chick lungs.	48
Figure 8. Characterization of Claudin-8 and-10 expression in branching chick lungs.	49
Figure 9. Characterization of Claudin-14 in branching chick lungs and no primary control.	50
Figure 10. Characterization of Claudin-5 expression in epithelial and endothelial cells of branching chick lungs.	51
Figure 11. Chick lung explants cultured with 5% chicken serum and 5% FBS or 10% FBS grow similarly.	53
Figure 12. Cultured E5 chick lung explants have a more complex structure than E4 lungs.	54
Figure 13. Chick lung explants exhibited improved growth when cultured on inserts with 8 μm pore filters than on those with 0.7 μm pores.	54
Figure 14. C-CPE-soaked beads do not affect primary branching in explant cultures of chick lungs.	55
Figure 15. Bisected E5 chick lungs had distinct branching patterns in explant culture.	56
Figure 16. Cauterizing E5 chick lungs did not affect development of the explant.	56
Figure 17. Cultured E11.5 mouse lung explants branched less and had more variability than E12.5 explants.	57
Figure 18. C-CPE affected growth of E5 chick lungs grown in explant culture.	59
Figure 19. Chick lung explants cultured with 800 $\mu\text{g}/\text{ml}$ of C-CPE have a smaller lumen perimeter and lumen area compared to controls.	60
Figure 20. C-CPE localizes to the apical side of epithelial cells in treated lungs.	61
Figure 21. C-CPE treatment did not affect αSMA in chick lung explants.	62
Figure 22. Preliminary results suggest removal of Claudin-3 in C-CPE-treated chick lung explants.	62
Figure 23. C-CPE treatment did not affect branching in E12.5 mouse lung explants.	63
Figure 24. C-CPE treatment affected Claudin-3 localization in cultured mouse lungs.	64

List of tables

Table 1. Restriction enzyme and RNA polymerase for the generation of chick *Claudin* antisense riboprobes. 35

Table 2. Summary of mRNA and protein expression for a subset of claudins in the chick lung at E4, E5 and E6. 51

List of abbreviations

°C: Degrees Celsius
αSMA: alpha smooth muscle actin
μg: Microgram
μl: Microliter
μm: Micrometer
BCIP: 5-bromo-4-chloro-3-indolyl-phosphate
BMP: Bone morphogenetic protein
BSA: Bovine serum albumin
C-: Carboxyl-terminal region
Ca²⁺: Calcium ion
C-CPE: Carboxyl-terminal region of the *Clostridium perfringens* enterotoxin
cDNA: Complementary deoxyribonucleic acid
Cl⁻: Chloride ion
Cldn: Claudin
CO₂: Carbon dioxide
CPE: *Clostridium perfringens* enterotoxin
DNA: Deoxyribonucleic acid
DMEM/F12: Dulbecco's Modified Eagle Medium: Nutrient Mixture F-12
DTT: Dithiothreitol
E: Embryonic day
EDTA: Ethylenediaminetetraacetic acid
FBS: Fetal bovine serum
FGF: Fibroblast growth factor
FGFR: Fibroblast growth factor receptor
GDNF: Glial cell-derived neurotrophic factor
GST: Glutathione-S-transferase
GUK: Guanylate kinase
h: Hour
HCV: Hepatitis C virus
JAM: Junctional adhesion molecule
K⁺: Potassium ion
KCl: Potassium chloride
kDa: Kilodalton
kPa: Kilopascal
LB: Lysogeny broth
MAPK: Mitogen-activated protein kinase
MDCK: Madin-Darby canine kidney
ml: Millilitre
MLCK: Myosin light chain kinase
mm: Millimetre
mM: Millimolar
mRNA: Messenger ribonucleic acid
MUPP: Multi-Post-synaptic density 95/*Drosophila* discs large/Zonula occludens-1 domain protein
N-: Amine-terminal region
Na⁺: Sodium ion
Na²HPO₄: Sodium phosphate dibasic

NaCl: Sodium Chloride
NBT: Nitro blue tetrazolium chloride
ng: Nanogram
NGS: Normal goat serum
O₂: Dioxygen
OCT: Optimum cutting temperature
P: Postnatal day
PALS: Protein associated with Lin-7
PATJ: Protein associated with Lin-7-associated tight junction
PBS: Phosphate buffered saline
PBT: Phosphate buffered saline plus 0.1% Tween-20
PDZ: Post-synaptic density 95/*Drosophila* discs large/Zonula occludens-1
PFA: Paraformaldehyde
pH: Potential of hydrogen
Ret: Rearranged during transfection
Rho: Ras homolog gene family
RNA: Ribonucleic acid
RNAi: Ribonucleic acid interference
rpm: Revolution per minute
fRT-PCR: Reverse transcription polymerase chain reaction
SD: Standard deviation
SDS: Sodium dodecyl sulfate
SH3: Src-homology3
SHH: Sonic hedgehog
SPRY: Sprouty
SSC: Saline sodium citrate buffer
STE: Sodium chloride-Tris-Ethylenediaminetetraacetic acid
TCA: Trichloroacetic acid
Tris-HCl: Tris(hydroxymethyl)aminomethane hydrochloride
U: Units
Wnt: Wingless integration site
WT: Wild type
ZO: Zonula occludens

Acknowledgements

I would like to start by thanking my co-supervisors Dr. Indra Gupta and Dr. Aimée Ryan. It was a pleasure being a part of your labs. Thank you for the chance that you have given me to do research with you. You have always been there to hear about my worries, to guide me through my project, to discuss results and future experiments. Thank you also for always taking the time out of your busy schedules to read my texts and help me prepare presentations. This helped improve my writing and my presentation skills. Your advice was always relevant, and it made me think about my project in other ways. I would like to thank also the members of my committee meeting Dr. Daniel Dufort and Dr. Benjamin Smith for providing great advice on how I can improve my project. I am thankful to Dr. Loydie Majewska and the members of her lab who always asked good questions during the Monday lab meetings. I greatly benefited from the suggestions that emerged from these meetings.

In the past two years, I have met wonderful people which became friends along the way. They helped me through the various obstacles of research and was always there to give me a hand when I was lost. Thank you, Enrique, for everything you have done for me. You are a model of hard work, determination and (almost) infinite knowledge. I was lucky I could count on you during these past years. Thank you, Amanda B., for all the techniques you showed me and the many questions you answered when I needed your expertise. Merci Jasmine pour ta patience et ton aide pour toutes ces expériences qui ont été grandement améliorées grâce à tes nombreux conseils. Thank you, Maria, for the *in situ* probes, for helping with the *in situ* experiments and for these moments of laughter. Thank you, Vasikar, for all the discussions on my project and on science in general which helped improve my project. I would like to thank also Fatima, Amanda V., Jenna, Liz, and Dareen for your valued help with your questions and suggestions. It greatly improved my project. A special thanks to all the undergraduate and summer students which helped make the lab a better place.

Also, I would like to acknowledge the help of the employees of the different platform at the RI-MUHC. I want to thank especially the employees of the Molecular Imaging Platform Dr. Min Fu and Shi-Bo Feng which trained me to use the confocal microscope and were always available to help me improve my pictures.

Finalement, j'aimerais remercier ma famille et mes amis pour votre support et vos encouragements pendant ces deux dernières années. Merci Charlie, toi qui crois toujours en moi

et qui a toujours le mot parfait pour me faire voir la lumière lorsque je suis persuadé que tout va mal. Je t'aime.

Format of the thesis

This traditional master's thesis was written according to the guidelines and format stated by Graduate and Postdoctoral Studies, McGill University.

Contribution of authors

The candidate prepared and performed all the experiments presented here. The candidate together with his two supervisors, Aimée Ryan and Indra Gupta, were involved in experimental design, analysed the data and edited all the content in this thesis.

CHAPTER 1: Introduction

1.1 Tight junctions

Tight junctions are the most apical junctional protein complexes that are established between the membrane of adjacent epithelial and endothelial cells. They are organized in the form of strands across the membrane. These junctions are particular because they are responsible for the permeability or 'tightness' of the tissue. Their main function is to regulate the passage of ions and solutes through the paracellular pathway (Figure 1). In fact, some transmembrane tight junction proteins restrict the passage of specific groups of molecules whether it is by their size or by their charge (reviewed by Gupta & Ryan (2010)). In certain tissues, for example in the bladder, tight junctions act more as a barrier by blocking paracellular flow (Krause *et al.*, 2008). In other tissues like the kidney nephron, tight junctions are regulators of the reabsorption of water and ions (reviewed in Szaszi & Amoozadeh (2014)). In the blood-testis barrier, the tight junctions have a major role in isolating the germ cells from the bloodstream. It allows the tight junctions to control the passage of ions and solutes necessary for the development of the germ cells in their microenvironment (reviewed in Mruk & Cheng (2015)). The role of the tight junctions in these different tissues suggests that the permeability of tight junctions depends on the tissue in which they are localized. Tight junctions are also responsible for regulating epithelial cell adhesion. They have strong cell-adhesion activities which allow them to form 'kissing points'. These structures form where the membrane of adjacent epithelia are in contact with each other (Kubota *et al.*, 1999). Tight junctions also have a role in maintaining the apical-basal polarity by segregating the membrane proteins specifically expressed at the apical or the basolateral side of the cell (Balda *et al.*, 1996).

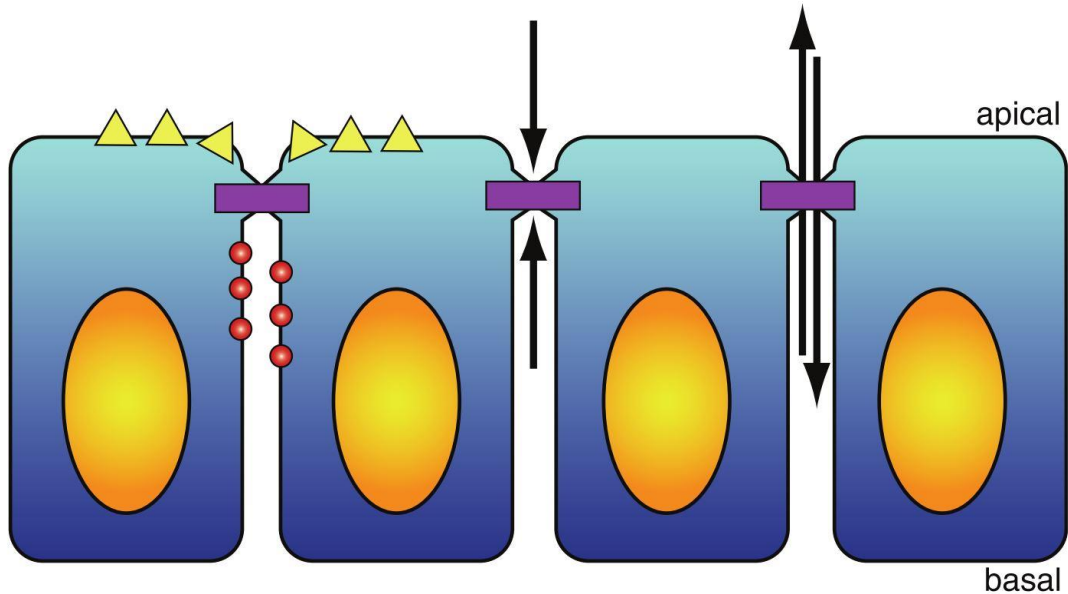


Figure 1. Schematic of the different functions of tight junctions.

Tight junctions have multiple functions. They maintain the cell's apical-basal polarity by segregating the proteins expressed on the cell membrane apical surface (yellow triangles) from the proteins expressed on the basolateral membrane surface (red circles). The tight junctions also act as barriers in specific tissues by blocking transfer through the paracellular pathway. Finally, they regulate the paracellular passage of ions and solutes by differentially selecting for charge and size. These properties are determined by the different tight junction proteins present in the various tissues. The figure is from Gupta & Ryan (2010).

Tight junction barrier permeability is controlled by different protein families that constitutes the tight junction complex. Transmembrane proteins such as claudins, occludin and junctional adhesion molecules (JAMs) (Figure 2) interact with each other on the same membrane and on the adjacent cell membrane to regulate the cell layer's permeability (Cording *et al.*, 2012). Claudins are the only transmembrane proteins necessary for tight junction formation (Furuse *et al.*, 1998). Beneath the plasma membrane, transmembrane proteins interact with scaffolding proteins at the cytoplasmic plaque. They are necessary to link the transmembrane proteins to other structural or signaling proteins. For example, the Zonula occludens proteins, which include ZO-1, ZO-2 and ZO-3, interact with each other and with the C-terminal tail of claudins through different protein domains. In fact, specific PSD-95/discs-large/Zonula occludens-1 (PDZ) domains are known to interact with the C-terminal tail of most claudins (Itoh *et al.*, 1999). PDZ domains are common structural domains which are present in many scaffolding proteins. Their main role is to link different proteins together and anchor them to the cytoskeleton. Scaffolding proteins also

interact directly with the actin cytoskeleton indirectly linking the claudins to the actin cytoskeleton (Figure 2) (Fanning *et al.*, 1998, Wittchen *et al.*, 1999). Using fluorescence recovery after photobleaching, Van Itallie *et al.* showed that the interactions between claudins and ZO-1, and between ZO-1 and actin, are highly dynamic with their association occurring at irregular intervals (Van Itallie *et al.*, 2017). Even though my project focuses on claudins, the other proteins of the complex are also important to consider because their interaction with claudins affects different molecular and cellular processes. Indeed, the effects seen by the removal of claudins from the tight junctions might be caused by the decrease in interactions with the proteins of the tight junction complex.

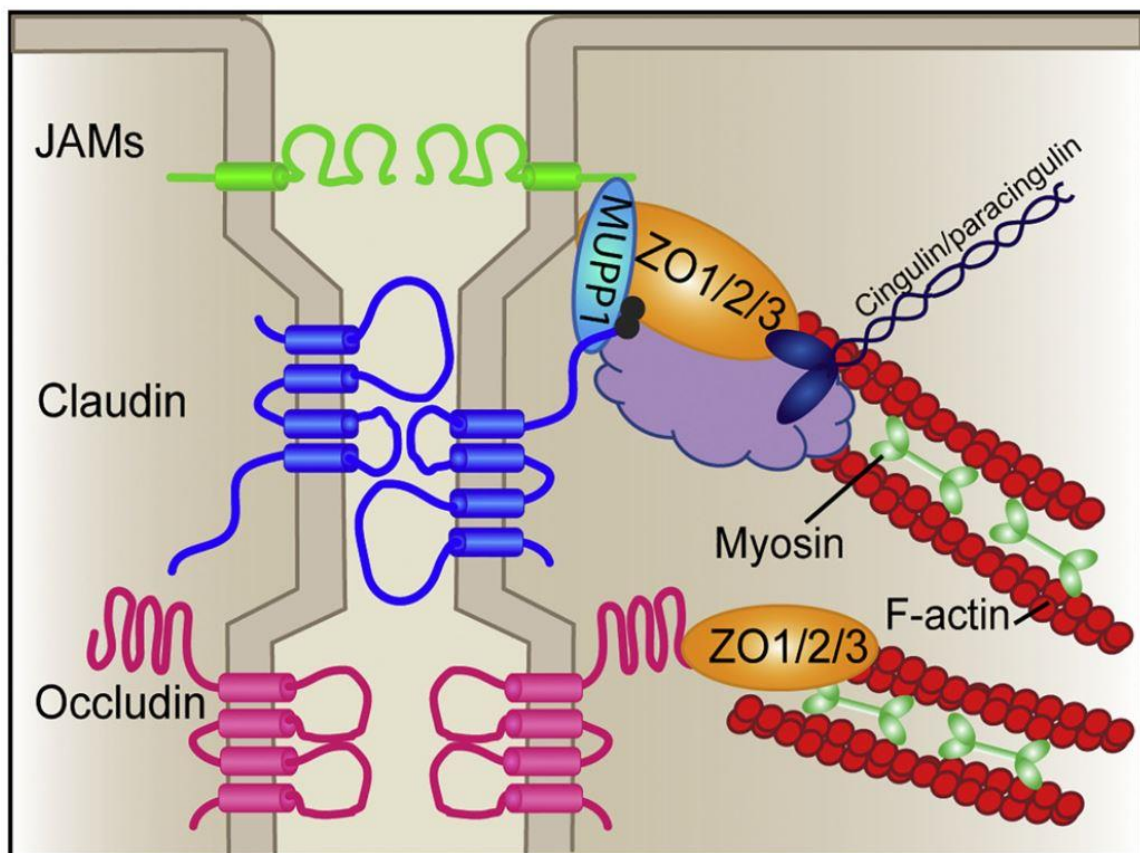


Figure 2. Schematic of tight junction protein complex.

Tight junctions are protein complexes formed by the assembly of multiple protein families. The main transmembrane proteins in tight junctions are claudins, occludin and junctional adhesion molecules (JAMs). They interact with scaffolding proteins such as ZO proteins, MUPP1, cingulin and paracingulin which link them to the actin cytoskeleton. The figure is from Gamero-Estevéz *et al.* (2018).

1.1.1 Tight junction proteins

1.1.1.1 Claudins

Claudins are a family of integral membrane proteins and have a prominent role in tight junction complexes. They have four transmembrane domains, two extracellular loops, a short intracellular loop and their N- and C- termini are in the cytoplasm (Figure 3). It is mostly the two extracellular loops that define the barrier properties of the different claudin members. The first extracellular loop sequence is very variable between claudins and the charged amino acids located in this loop determine the ionic specificity of the claudin (Colegio *et al.*, 2002). The second extracellular loop is responsible for the oligomerization between the claudin units, which is the interaction that allows the formation of the strands across the cell membrane. The second extracellular loop of a subset of claudins also includes a *Clostridium perfringens* enterotoxin (CPE) binding site (Figure 3). The C-terminal domain is important to interact with intracellular proteins. It includes a PDZ-binding domain which allows scaffolding proteins such as the Zonula occludens proteins to interact with claudins (Figure 3). The C-terminal domain is also often modified by post-translational modifications. These modifications influence the stability, the structure and the localization of the claudins. They can also affect the capacity of the claudins to interact with other proteins (Tanaka *et al.*, 2005). Claudin family members interact with each other to form the tight junctions. These interactions take place between claudins on the same membrane (*cis*-interactions) or with claudins on the membrane of neighbouring cells (*trans*-interactions). The transmembrane domains of claudins are important for the dimerization of claudins to form *cis*-interactions or 'strands' along the plasma membrane (Van Itallie *et al.*, 2011). However, the *cis*-interaction between claudins also involves extracellular loops (Schlingmann *et al.*, 2015).

Claudins play an important role in regulating the permeability of several tissues, including the intestines, the bladder and the kidneys (reviewed in Krause *et al.* (2008)). More than 20 members have been discovered in vertebrates and this allows many possible combinations that dictate permeability.

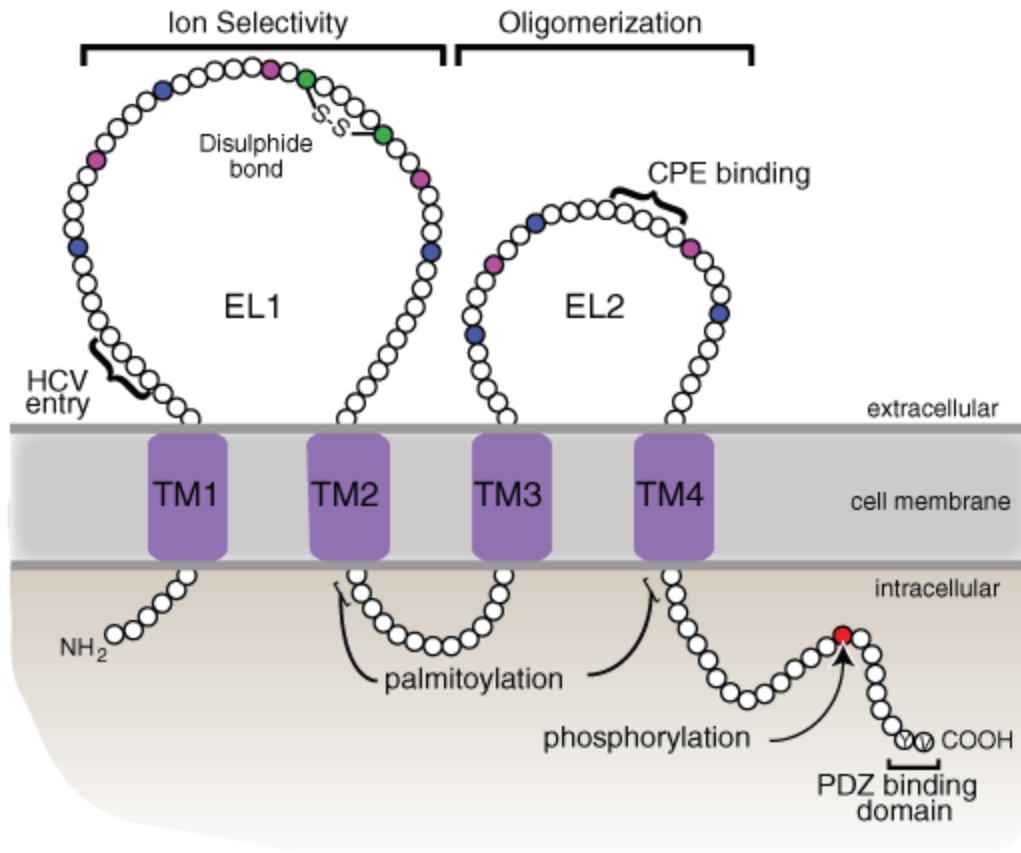


Figure 3. Schematic of claudin protein.

Each claudin family member has a similar structure that consists of two extracellular loops, four transmembrane domains and cytoplasmic N- and C- termini. The first extracellular loop is mainly responsible for the charge selectivity of the ions and molecules which can traffic through the paracellular pathway. The first extracellular loop of at least Claudin-1 also includes a Hepatitis C virus (HCV) receptor site. The second extracellular loop is important for the establishment of claudin complexes formed by the oligomerization of multiple claudin members. A subset of claudins also have a *Clostridium perfringens* enterotoxin (CPE) binding site on the second extracellular loop. The C-terminal domain is important to interact with intracellular proteins. It includes a PDZ binding domain which allows scaffolding proteins such as ZO-1 to interact with claudins. These proteins link the claudins to other proteins interacting with the actin cytoskeleton. The figure is from Gupta & Ryan (2010).

Interaction between two identical claudins is considered homotypic and when the interaction is between two different claudins, it is classified as heterotypic. Most of the time, claudins have preferred partners in their heterotypic interactions. For example, Claudin-3 is known to interact

with Claudin-4 in a *cis*-interaction, but not in *trans* (Daugherty *et al.*, 2007). Also, Claudin-1 can associate with Claudin-3 in a *trans*-interaction (Furuse *et al.*, 1999).

Claudins are also classified by their ability to form pores or to seal the tight junction. This is usually determined by their capacity to increase or decrease transepithelial electrical resistance when overexpressed in a cell line. Transepithelial electrical resistance is the measurement of the resistance of an electric current passing through an epithelial cell layer. It has been used to assess tight junction permeability. A high transepithelial electrical resistance indicates that there is more resistance in the cell layer meaning that the cells are closer to each other and that their ability to let ions to pass through is affected. If a claudin that is overexpressed in a low resistance cell line increases the transepithelial electrical resistance, the claudin is considered a sealing claudin. Sealing claudins include Claudin-1, -3, -5, -7, -11 and -18, while pore-forming claudins include Claudin-2, -4, -8, -10, -14, -15, -16 and -19 (Hou *et al.*, 2013). However, this change in transepithelial electrical resistance depends on the interaction of the claudin with the tight junction proteins already in the specific tissue. Indeed, the functional classification of claudins is not straightforward because they have different functional characteristics depending on their interacting partner and the microenvironment. Claudins can also control the permeability of the paracellular pathway according to the charge of the molecule by forming anion or cation specific pores or barriers. For example, when Claudin-4, which is a barrier claudin, is overexpressed in Madin-Darby Canine Kidney (MDCK) cells, the permeability of Na⁺ is decreased compared to the Cl⁻ permeability (Van Itallie *et al.*, 2001). The relationship between the claudin interaction partner in *cis* and in *trans* can also determine whether claudins form a cation or anion specific paracellular pore or barrier. For instance, Claudin-4 and Claudin-8 need to interact to form a Cl⁻ channel in the kidney collecting duct (Hou *et al.*, 2010). These data show that the claudin family members have different roles in tissue permeability suggesting that the effect of altering claudin localization or expression would depend on the targeted claudins and the claudins that remain in the tight junction. It would be challenging to determine if the effect is due to the absence of this claudin in the tight junction or due to the elimination of its interaction with the other claudins.

Claudins can also undergo post-translational modifications. These modifications can alter the function and regulate the interactions and localization of the claudin. Different classes of post-translational modifications are observed in claudins with phosphorylation being the most

common modification detected in claudins. It consists of the addition of a phosphoryl group to a serine, a threonine or a tyrosine residue of a protein. In the claudin proteins, phosphorylation sites are often localized in the C-terminal tail (Liu *et al.*, 2016). Phosphorylation of claudins can affect different characteristics of the protein and the effects are dependant on the residue and the claudin family member. For example, phosphorylation of Claudin-4 at Tyr208 located in the C-terminal tail affects the interaction of the claudin with ZO-1, decreasing its localization to the tight junction (Tanaka *et al.*, 2005). However, phosphorylation of Ser208 in Claudin-2 increases its retention in the membrane of MDCK cells (Van Itallie *et al.*, 2012).

Claudin residues can also be palmitoylated. Palmitoylation is the addition of fatty acids to specific residues, mainly cysteines. In all claudins, next to the second and the fourth transmembrane domains, there are two cysteine residues with a palmitoylation motif (Van Itallie *et al.*, 2005). Claudin-14 needs the palmitoylation at these specific residues to properly be localized at the tight junction (Van Itallie *et al.*, 2005). Other post-translational modifications such as ubiquitination, SUMOylation and glycosylation have been observed or predicted in claudins but are less common than the phosphorylation and the palmitoylation.

1.1.1.2 Occludin

Occludin is an integral membrane protein localized in tight junctions. It was the first tight junction transmembrane protein to be identified (Furuse *et al.*, 1993). Its structure consists of 4 transmembrane domains, two extracellular loops and cytoplasmic N- and C- termini. Each domain has a distinct function. For example, it has been shown that the extracellular loops have roles in occludin localization and in maintaining tight junction stability (Balda *et al.*, 2000). The C-terminus of occludin interacts with the guanylate kinase (GUK) domain of ZO-1 (Schmidt *et al.*, 2004). This interaction has been shown to be important for occludin localization at the plasma membrane (Furuse *et al.*, 1994). Knockdown of ZO-1 in MDCK cells delayed occludin recruitment to the membrane while the occludin knockdown did not affect ZO-1 recruitment (Odenwald *et al.*, 2017).

Numerous papers have confirmed that occludin has a role in regulating tight junction paracellular permeability. When occludin was overexpressed in MDCK cells, there was an increase in the transepithelial electrical resistance (McCarthy *et al.*, 1996). Despite that, occludin is not necessary for the formation of tight junctions. In fact, an occludin mouse knock-out showed no

morphological differences in tight junction strands. Nevertheless, different epithelial tissues in the occludin mouse knock-out showed a decline in tight junction integrity, suggesting a role in tight junction maintenance rather than tight junction formation (Saitou *et al.*, 2000).

1.1.1.3 Junction adhesion molecules

Junction adhesion molecules (JAMs) are part of the immunoglobulin superfamily. They are expressed by platelets, leukocytes, endothelial cells and epithelial cells. Their structure consists of only one transmembrane domain, two extracellular immunoglobulin-like domains and a cytoplasmic tail that contains a PDZ binding-domain sequence (Ebnet *et al.*, 2004). JAMs are known to have two main functions: they regulate the interaction between endothelial cells, platelets and leukocytes, and they maintain tight junction integrity. Briefly, when JAM-A, a member of the JAM family, was ectopically expressed in fibroblasts, tight junction strands did not form. This suggests that JAMs are not sufficient for tight junction formation (Itoh *et al.*, 2001). The JAMs' PDZ domain-binding sequence interacts with proteins of the tight junction cytoplasmic plaque, including ZO-1 (Bazzoni *et al.*, 2000) and MUPP1 (Hamazaki *et al.*, 2002).

1.1.1.4 Zonula occludens family of tight junction proteins

The Zonula occludens family of tight junction proteins consists of three proteins: Zonula occludens-1 (ZO-1), Zonula occludens-2 (ZO-2) and Zonula occludens-3 (ZO-3). These proteins are located in the tight junction cytoplasmic plaque. They all contain three PDZ domains, a Src-homology3 (SH3) domain and a GUK domain (Itoh *et al.*, 1999). PDZ domains can interact with many different proteins such as claudins, ZO-2 and JAM-A (Itoh *et al.*, 1999, Ebnet *et al.*, 2000). The GUK domain can bind to occludin (Fanning *et al.*, 1998). ZO proteins are considered scaffolding proteins because they link the C-terminus of the tight junction transmembrane proteins to the actin cytoskeleton (Fanning *et al.*, 1998). ZO-1 is not essential for tight junction formation. This was illustrated by the presence of tight junction strands in the Eph4 cell line, a mouse epithelial cell line, which was knocked out for ZO-1. However, in the absence of ZO-1, there was a delay in junction assembly illustrated by the fact that Claudin-3 and occludin strands were more fragmented in ZO-1 depleted cells compared to control. This phenotype was then rescued by exogenous expression of ZO-1 (Umeda *et al.*, 2004). Because ZO-1 is expressed at the

cytoplasmic plaque of the tight junctions, we use it as a tight junction marker when doing immunofluorescence. However, ZO-1 is also expressed in the adherens junctions, which is another junctional complex localized more basal compared to the tight junctions (Farquhar & Palade, 1963). Despite this, it is still a good tool to highlight the positions where the cells establish junctions. ZO-3 has been shown to bind to ZO-1 and the C-terminal tail of occludin, but not with ZO-2 (Haskins *et al.*, 1998). ZO-3 can also bind directly to the actin cytoskeleton (Wittchen *et al.*, 1999).

1.2 *Clostridium perfringens* enterotoxin

To study the role of multiple claudins, a tool called the C-terminus of *Clostridium perfringens* enterotoxin (C-CPE) is often used. C-CPE is derived from CPE which is a toxin secreted by the *Clostridium perfringens* bacteria that causes food poisoning symptoms associated with *C. perfringens* ingestion (McClane, 2001). CPE binds to the second extracellular loop of Claudin-3, -4, -6, -7, -8 and -14 (Fujita *et al.*, 2000) and drives the epithelial cell to undergo cell death through its cytotoxic N-terminal domain (Katahira *et al.*, 1997). The mechanism which is responsible for cell death starts when CPE binds to the specific claudins to form a complex. Six of these CPE-claudin complexes oligomerize to form a large prepore complex. This complex inserts itself into the membrane which forms a pore that let solutes like calcium pass through the membrane. This influx of calcium into the cytoplasm cause the cell to undergo oncosis or apoptosis through the activation of different mechanisms. The N-terminal domain of CPE is what causes the formation of the pore which induces the cytotoxic effect. By using only the C-terminus of CPE, the protein still binds to the targeted claudins and removes them from the tight junctions but does not generate cell death (Sonoda *et al.*, 1999).

CPE-sensitive claudins were identified by transfecting fibroblasts lacking tight junctions with plasmids containing the sequence of a single claudin. These fibroblasts expressing single claudins were then treated with CPE. Considering that CPE causes apoptosis by binding to specific claudins, the claudins expressed by fibroblasts undergoing apoptosis were considered as CPE-sensitive claudins (Fujita *et al.*, 2000). This is important because the affinity of CPE on a tissue with endogenous claudins might be different than in a fibroblast expressing a single claudin. In fact, in neural and non-neural ectoderm tissue treated with C-CPE, every CPE-sensitive claudin was

affected except Claudin-14 (Baumholtz *et al.*, 2017). This could be due to the fact that the different CPE-sensitive claudins bind to CPE with various affinities (Fujita *et al.*, 2000). When C-CPE is in contact with a tissue containing multiple claudins, it might bind preferentially to the claudins that have a higher affinity for the peptide. Other hypotheses which explain why Claudin-14 is not affected in certain tissues include the fact that a Claudin-14 may have a higher affinity toward its usual binding partner than toward C-CPE. Claudin-14 may also be expressed at a more basolateral position compared to other claudins and would not be in contact with C-CPE. Post-translational modifications which change the claudin structure might be another reason why the effect of C-CPE is different between tissues.

It is also important to mention that even though C-CPE only affects the claudins which have a CPE-binding site in their sequence, the removal of these claudins can also affect the localization of their claudin partners in *cis* and in *trans*. This is important to consider because it is not known how these interactions are reorganized when the cells are treated with C-CPE.

To study the role of claudins in different tissues, I used the C-CPE protein because it specifically binds to the sensitive claudins allowing for the targeted removal of multiple claudins at the same time. This is important because several claudins have overlapping functions and the removal of only one claudin might be compensated by another claudin member. Other groups have used C-CPE to study claudins. For example, Moriwaki *et al.* used GST-C-CPE to study claudin function in mouse blastocysts (Moriwaki *et al.*, 2007). Mouse blastocysts contains Claudin-4, -6, -7 and -12. They showed that mouse blastocysts cultured with C-CPE removed Claudin-4 and -6 from the trophoectoderm, the first epithelium produced during mammalian development, but it did not remove Claudin-7. These embryos had an absent or a smaller blastocoel cavity compared to the controls. This demonstrates that GST-C-CPE is useful to target multiple claudins and is a powerful tool to study the role of claudins during development. It also reveals that even though Claudin-7 has a relatively high affinity to C-CPE, it was not removed from the tight junctions after C-CPE treatment. This further shows that the C-CPE effect on claudin removal is dependent on the tissue.

1.3 Claudins during development

With C-CPE as a tool to target multiple claudins, their function can be studied in different tissues and organisms. Claudins have important roles during development. During the gastrulation stage of the chicken embryo, altering the expression of Claudin-1 and Claudin-10 leads to the randomization of heart looping (Simard *et al.*, 2006, Collins *et al.*, 2015). Also, claudins are important to control the microenvironment by regulating the paracellular transport which is necessary for the establishment of hydrostatic pressure differentials. This is essential for the formation a fluid-filled lumen like in the neuroepithelium of the zebrafish brain where Claudin-5a promotes lumen formation (Zhang *et al.*, 2010). Claudins are also essential during neural tube closure. The removal of Claudin-3, Claudin-4 and Claudin-8 from the tight junctions of chicken embryos during neural tube closure results in neural tube defects. It was shown that they regulate convergent extension and cell shape, critical processes during neural tube closure (Baumholtz *et al.*, 2017).

Recent data have revealed a possible role for claudins during the branching of different organs. In fact, claudins are expressed during early stages of development of organs like the lung, the kidney and the submandibular gland. Several studies analysing the expression of a subset of claudins in different branching organs have been published in the past few years and an overview of these papers is found in the paragraph on branching morphogenesis (section 1.4).

1.3.1 Mouse claudin knock-out and knockdown assays

Single claudin knock-out mouse lines have been produced for the majority of the members of the claudin family and only a few have lethal or severe phenotypes. This is surprising considering the fact that claudins are necessary for several key processes during development. This suggests that claudins have overlapping functions: the removal of a claudin is compensated by the overexpression or underexpression of other claudin members (reviewed in Gupta & Ryan (2010)). However, the phenotypes of the claudin knock-out mice can be studied and the phenotypes can be compared to wild type mice to determine the role of the specific claudin in a certain tissue. For example, if differences in the permeability of a tissue are observed in the knock-out mice compared to wild type mice, this can indicate the function of the knocked out claudin in this

specific tissue. Below is a brief overview of the different mouse claudin knock-outs, knockdowns and overexpression assays that have been performed and the resulting phenotypes.

Claudin-1-deficient mice are born with a wrinkled appearing skin and they die within the first postnatal day due to dehydration caused by epidermal barrier defects in the skin. This was shown by measuring the transepidermal water loss in newborns (Furuse *et al.*, 2002).

Claudin-2-deficient mice have a normal appearance, growth and behavior. Their kidneys also look morphologically normal, but the cells in the proximal tubule of the nephron had decreased transepithelial reabsorption of Na⁺, Cl⁻ and water (Muto *et al.*, 2010). No other organs were studied.

Claudin-3-deficient mice have a normal appearance and behavior and histological analysis shows no difference in the kidney nephron compared to wild type (Kerr *et al.*, 2015). However, no functional analysis of the different organs was assessed.

Claudin-4-deficient mice show no embryonic phenotype and develop normally until adulthood. However, a diminution of alveolar fluid clearance and a higher permeability to small solutes was observed in the lungs. Claudin-4 knock-out mice are also more susceptible to lung injury compared to wild type (Kage *et al.*, 2014).

Claudin-5-deficient mice develop normally, and no endothelial defects are observed in histologic analysis. However, an increase in blood brain barrier permeability against molecules smaller than 800 Da is observed (Nitta *et al.*, 2003).

Claudin-6-deficient mice are viable and fertile and do not present any obvious phenotype (Anderson *et al.*, 2008).

Claudin-7-deficient mice are viable until postnatal day 12 when they die of renal salt wasting and chronic dehydration (Tatum *et al.*, 2009). Intestinal phenotypes like mucosal ulcerations and inflammation are also observed in Claudin-7-deficient mice (Ding *et al.*, 2012).

Claudin-11 is different than other claudins in the fact that it is expressed in organs where no or few other claudins are expressed. In fact, it is expressed in the oligodendrocytes of the central nervous system (Bronstein *et al.*, 1997), the Sertoli cells in the testis (Morita *et al.*, 1999) and in a basal cell layer of the cochlea, a cavity of the ear (Kitajiri *et al.*, 2004). This is why Claudin-11-deficient mice have stronger phenotypes. In fact, these mice have no tight junction strands in the

oligodendrocytes and show hindlimb weakness (Gow *et al.*, 1999). Claudin-11-deficient mice also lack tight junction strands in the Sertoli cells and the males are sterile (Gow *et al.*, 1999). The study of the cochlea showed that in Claudin-11-deficient mice, the basal cells of the cochlea also lack tight junction strands and these mice exhibit deafness (Gow *et al.*, 2004).

Claudin-14-deficient mice are deaf due to the rapid degeneration of hair cells in the cochlea. It has been suggested that Claudin-14 is necessary for the proper ionic composition in the cochlear fluid and a perturbation in this fluid composition causes the degeneration of the hair cells (Ben-Yosef *et al.*, 2003).

Claudin-15-deficient mice develop normally but have an upper small intestine that is 2 times larger in length and diameter than wild type. Cells in the intestinal crypt have a higher proliferation rate in Claudin-15-deficient mice than in wild type mice (Tamura *et al.*, 2008).

Claudin-16 was knocked down in mice using RNA interference (RNAi). Claudin-16-deficient mice show less cation selectivity than wild type animals in the thick ascending limb of the nephron kidney (Hou *et al.*, 2007).

Claudin-18-deficient mice develop normally. Analysis of the lung revealed no apparent lung dysfunction, but there were differences in permeability and alveolar fluid clearance. In fact, alveolar epithelial cells layer of Claudin-18 knock-out mice showed higher permeability to K^+ , Na^+ and Cl^- and a higher alveolar fluid clearance. Claudin-3 and Claudin-4 expression was higher in the lung epithelial cells of Claudin-18 knock-out animals compared to wild type animals while occludin expression was decreased in knock-out mice (Li *et al.*, 2014). Impaired alveolarization and an increase in lung injury was also observed in 4 weeks old Claudin-18-deficient mice (LaFemina *et al.*, 2014).

Claudin-19-deficient mice have abnormal behaviors associated with defects in the peripheral nervous system but not the central nervous system. Further analysis of the axons of the peripheral nervous system revealed that although Schwann cells looked morphologically normal, they lacked tight junctions (Miyamoto *et al.*, 2005).

1.4 Branching morphogenesis

Branching morphogenesis is a critical developmental process that is critical for the formation of many organs, including the lung, kidney and mammary gland. Studying the different mechanisms by which a single tubule forms a complex three-dimensional structure is fundamental to understand the process of developing a functional embryo. For the purpose of this report, branching morphogenesis is defined more specifically as all the mechanisms necessary for an epithelial cell layer to change shape and form additional tubules. This process eventually forms a complex branched network. Branching morphogenesis is important because many organs like the kidney, the lung, the salivary glands and the mammary gland contain a branched epithelium. Each organ uses different branching patterns to form its network. The salivary glands use a clefting branching pattern: a bud will separate itself into several smaller buds by the formation of clefts in the main bud (Patel *et al.*, 2006). The kidney branches through multiple rounds of bifurcation and trifurcation of a single tubule (Watanabe & Costantini, 2004).

For my project, I focus on lung branching. In the lungs, the tubules go through different types of branching to form the mature organ: domain branching, planar bifurcation and orthogonal bifurcation. Domain branching occurs through the formation of buds along the length of a tubule. Planar bifurcation represents the bifurcation of a tubule on the same plane as the plane of the previous bifurcation while orthogonal bifurcation occurs orthogonally from the previous bifurcation.

The molecular mechanisms that control lung branching have some similarities with kidney branching. For example, in both organs, fibroblast growth factors (FGFs) have a predominant role and are expressed by the mesenchymal cells to initiate branching. The FGF signal activates the mitogen-activated protein kinase (MAPK) cascade and regulates different downstream proteins that affect diverse cellular mechanisms (Varner & Nelson, 2014). BMP4 and Wnt proteins have major roles in both organs. However, there are several differences between the two organs that must be considered. First, they come from different germ layers: lungs originate from the endoderm, while the kidneys are formed from the intermediate mesoderm. The molecular mechanisms also have differences. For example, the main factor coming from the mesenchymal cells in the lungs is fibroblast growth factor 10 (FGF10), while for the kidney, the mesenchymal cells release glial-derived neurotrophic factor (GDNF) (Affolter *et al.*, 2009).

Claudins are expressed during the branching morphogenesis of multiple organs. Claudin-3 protein is expressed in the epithelial cells of the mouse ureteric bud, the structure that will develop into a mature kidney. It is expressed during different period of its development including during branching morphogenesis (Haddad *et al.*, 2011). Also, previous results from my lab have shown that when a subset of claudins are removed from the tight junctions of embryonic mouse kidney explants using C-CPE, the number of terminal buds is decreased in C-CPE treated explants compared to control without affecting the overall size of the kidney (Khairallah, 2013). In the submandibular gland, Claudin-3 to -8, -10 and -11 proteins are expressed in the luminal epithelial cells during the branching of the mouse submandibular gland (Hashizume *et al.*, 2004). Claudin-1, -3, -4, -5, -7 and -11 were also expressed in epithelial cells of the branching human salivary glands while Claudin-2 expression was not observed (Lourenço *et al.*, 2007). With these data, a question arises: does the expression of claudins during the early branching of several organs indicate the necessity of claudins during the general branching morphogenesis process?

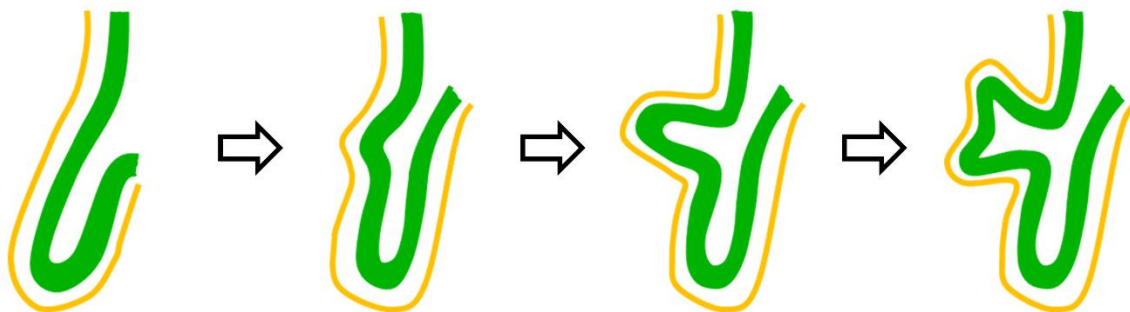


Figure 4. Schematic of the early steps in lung branching morphogenesis.

A representation of a bronchi with the mesothelium (orange line) and the endoderm (green line). The space between the orange and the green structures represent the mesoderm, a layer of mesenchymal cells. The space which is surrounded by the endoderm is the luminal space. Lung branching morphogenesis occurs by the formation of a bud caused by a change in shape of the endoderm. The bud elongates into the mesoderm and bifurcate to form two tubules.

1.5 Lung development

In this project, the mouse and the chick were used as animal models to study lung branching morphogenesis. To have a better overview of the steps needed to form a mature lung and to have more details on the stages used to study lung branching morphogenesis, the general chick and mouse lung development process are described below.

In the mouse, the primitive lungs go through five stages to form mature lungs: the embryonic, the pseudoglandular, the canalicular, the saccular and the alveolar stages. The lungs start developing at embryonic day (E) 9 when a bud emerges from the primitive foregut. The bud will branch into two structures that become the primary bronchi. Secondary buds will then form on the primary bronchi which will elongate and bifurcate (Figure 4). The lungs will go through the pseudoglandular stage (E13.5 to E16.5) when further branching occurs (tertiary bronchi and bronchioli). After, the terminal bronchioli elongate during the canalicular stage (E16.5 to E18.5). In the saccular phase (E18.5 to post-natal day (P) 0), the terminal bronchioli expand to form sacs surrounding the capillaries. Finally, during the alveolar stage (P0 to P18), alveoli are formed in the sacs to minimize the space between the airways and the capillaries, the site of gas exchange (Rackley & Stripp, 2012).

The beginning of avian lung development is similar to the mouse. It starts with the development of a bud from the primitive foregut that will form the trachea. This bud elongates and branches into two buds that will become the primary bronchi. At this step, avian lung development begins to differentiate from what is observed in mammals. The avian bronchi branch laterally into secondary bronchi while the mammalian bronchi are formed by a combination of lateral and bifurcated branching. The chick does not develop alveoli, but instead, gas exchange occurs with the capillaries through the parabronchi, a network derived from the anastomosis of the ventrobronchi and the dorsobronchi.

The molecular mechanisms responsible for bud formation and branching is similar between the two species (Kim *et al.*, 2013) and both could be driven by claudins. However, some differences in branching are observed between the two species. For example, apical constriction has been reported during chick lung early branching morphogenesis (Kim *et al.*, 2013). Apical constriction is the narrowing of the apical side of the cells forming the newly formed epithelial bud. This is due to the contraction of the fibers in the actin cytoskeleton. This mechanism, however, has not been reported in mammalian lung branching. Unlike chick lungs, α smooth muscle actin (α SMA) has an important role in mouse lungs branching morphogenesis. It is known to accumulate around the newly formed bud to guide the bud into bifurcating (Kim *et al.*, 2015). I used the chick and the mouse as animal models to determine if claudins have a role in lung branching morphogenesis because I would be able to observe if the role of claudins could be different depending on the branching morphogenesis mechanism.

1.5.1 Claudins during lung development

Multiple claudins are expressed in the lungs during its development. In the human lung, the Claudin-1, -3, -4, -5, -7 and -18 are expressed at the pseudoglandular stage (weeks 12-16 of gestation) and at later fetal stages (Daugherty *et al.*, 2004, Kaarteenaho *et al.*, 2010). Claudin-18 expression is also regulated throughout the fetal lung development. Claudin-18 expression increases during alveolarization which, in humans, happens in the few weeks before birth and extends until several months after birth (LaFemina *et al.*, 2014). A recent paper from Lewis *et al.* have looked at the pattern of expression of some claudins in mouse embryonic lungs. Using immunohistochemistry on sections, they showed that Claudin-3, -5, -6 and -7 are expressed in the epithelial cells of E12.5 mouse lungs (end of embryonic stage) while Claudin-1, -2, -4, -8 and -18 protein are not (Lewis *et al.*, 2018). Also, overexpression of Claudin-6 in mouse lungs causes an arrest in development at the canalicular stage (Jimenez *et al.*, 2016). This suggests that Claudin-6 is important for the normal development of the lung. However, Claudin-6-deficient mice do not have obvious defects in development (Anderson *et al.*, 2008). This shows the complexity in understanding the role of claudins during development. An imbalance in claudin expression may cause defects while the complete elimination of a claudin may not show any phenotype due to the recovery of the function by other claudins.

Previous work from my lab have examined the mRNA expression pattern of different claudins in the chick lung. Using RT-PCR and *in situ* hybridization, they found that *Claudin-1*, -3 and -10 mRNA are expressed in chick lungs during early development. More specifically, *Claudin-1* was expressed in the epithelial cells of embryonic chick lungs at E4 and E8 particularly in the bud tips (Simard *et al.*, 2005). *Claudin-3* was expressed in the early lung bronchus at E5, E7 and E10. Stronger expression could be seen at the tip of the buds at E7 and E10 like *Claudin-1*. *Claudin-10* was observed uniformly throughout the epithelial cells of the branching lung at E7 and E10 (Collins *et al.*, 2013). *Claudin-5* was also shown to be expressed in the vasculature surrounding the early chick lung bud at E4.5, E7 and E9 (Collins *et al.*, 2012).

Experiments affecting claudin expression were done to study their role during lung development. For example, Claudin-18 knock-out mouse have defects in the junctions between alveolar epithelial type I cells which results in impaired alveolarization (LaFemina *et al.*, 2014). Moreover, a transgenic mouse overexpressing Claudin-6 in developing lungs lead to delays in lung

morphogenesis. At E18.5, the transgenic mice lungs were in the early canalicular stage, while the control mice lungs were in the saccular stage (Jimenez *et al.*, 2016).

These results show that different claudins are expressed during lung development and that different claudins are necessary for complete lung organogenesis. Studies also support that the expression level of at least Claudin-6 and Claudin-18 are important factors in proper lung development.

1.6 Hypothesis and objectives

1.6.1 Hypothesis

The goal of my project is to determine the role of claudins during lung branching morphogenesis. Claudins play a major role in controlling paracellular flux of ions and solutes, but they are also necessary during development. Many developmental processes are dependent on claudins. A good example is how Claudin-3, -4 and -8 are required for neural tube closure (Baumholtz *et al.*, 2017). Previous results from my lab have also shown that when a subset of claudins were removed from the tight junction of embryonic mouse kidney explants using C-CPE, a reduced number of terminal bud tips were observed (Khairallah, 2013).

Because kidney and lungs are branched organs that have similarities in the molecular and morphological mechanisms that give rise to the branched structure, I **hypothesize that** claudins are necessary for early branching morphogenesis in the developing lung of both chick and mouse embryos.

1.6.2 Objectives:

1. Determine which claudins are expressed in the chick embryonic lungs during early branching morphogenesis.
2. Determine if C-CPE-sensitive claudins are required for branching morphogenesis in *ex vivo* cultured chick and mouse embryonic lungs.

CHAPTER 2: Materials and methods

2.1 Embryonic lung collection

Chick embryos were collected by incubating fertilized chicken eggs (Ferme GMS, Saint-Roch-de-l'Achigan, Québec) for the desired time (four days, five day or six days) at 39°C in an egg turner cabinet incubator (Brinsea). Scissors were used to cut a hole at the top of the egg and the embryo was removed with a holed spoon. Mouse embryos of the desired stage (E11 or E12.5) were collected from timed-pregnant CD1 female mice (Charles River Laboratory). Embryos were handled according to the Canadian Council on Animal Care guidelines.

Chick and mouse lung explants were collected by dissecting the embryos in phosphate-buffered saline (PBS) with 1% of penicillin and streptomycin. The head and the tail of the embryo were removed with forceps. The embryo was then cut longitudinally to take out its back. The heart was dissected out and the lungs were retrieved on the dorsal side of the heart. The oesophagus was then separated from the lungs and trachea, but to avoid damage to the lungs due to its fragility, the oesophagus was not removed from dissected E4 chick lungs.

2.2 Whole mount *in situ* hybridization

The cDNA sequences of the different claudin genes were cloned into pSC-A. The plasmids were linearized with an appropriate restriction enzyme (Table 1). If possible, an enzyme which does not produce a 3' overhang was chosen. To prepare the riboprobes, the gene transcription reaction was performed using 2 µl of 10x transcription buffer, 2 µl of 100 mM dithiothreitol (DTT), 0.5 µl of RNaseOUT™ (Thermo Fisher Scientific), 2 µl of 10x DIG RNA Labeling mix (Roche), 1 µg of linearized DNA and 1 µl of RNA polymerase (T3, T7 or SP6, see Table 1). RNase free water was added to reach 20 µl. This was incubated in a 37°C water bath for 2 hours. 1 µl of Rnase-free DNase (Promega) was added to the mix and it was incubated 10 minutes at 37°C. To precipitate RNA, 1 µl of 0.5 M of ethylenediaminetetraacetic acid (EDTA), 1.3 µl of lithium chloride (LiCl) and 55 µl of 100% ethanol was added to solution. This was incubated an hour at -80°C. It was then centrifuged at 4°C with a speed of 13,000 rpm for 30 minutes. The supernatant was discarded, and the pellet was left under the hood until it was dry. It was then resuspended in 20 µl of 0.1 M DTT and added to the hybridization solution. Hybridization solution consists of 50% formamide,

5x saline sodium citrate buffer (SSC) pH 5, 50 µg/ml yeast tRNA, 1% sodium dodecyl sulfate (SDS) and 50 µg/ml heparin. The amount of hybridization solution to add to the riboprobe is determined by running 1 µl of the riboprobe in 1% agarose gel against a solution with a known concentration to have a final concentration of approximately 1 µg/ml. The riboprobe was stored at -20°.

Collected embryonic chick lungs were fixed in 4% paraformaldehyde (PFA) in PBS for 12 minutes in ice. The samples were dehydrated by putting them in 10-minute washes of methanol:PBT solution with increasing concentration (1:3, 1:1, 3:1). It was then washed 10 minutes in 100% methanol. At this step, the samples could be stored at -20°C. The lungs were then rehydrated in 10-minute washes of methanol:PBT solution (3:1, 1:1, 1:3). They were put in two 5-minute washes of PBT. The samples were treated with a solution of 10 µg/ml proteinase K in PBT for a minute. The proteinase K solution was removed, and the samples were washed quickly with fresh solution of glycine in PBT (0.1 g of glycine in 50 ml of PBT). The glycine solution was replaced, and it was washed five minutes. The samples were fixed in 4% PFA plus glutaraldehyde (0.2% glutaraldehyde in PFA 4%) for 20 minutes on ice. They were then washed two times in PBT for 5 minutes at room temperature. After, the samples were washed five minutes in hybridization solution at room temperature. The solution was replaced by fresh hybridization solution and the samples were put in a 65°C water bath for an hour. The hybridization solution was replaced by the DIG labeled antisense or sense riboprobe and left overnight in the 65°C water bath. The samples were washed three times for 20 minutes at 65°C in a solution consisting of 50% formamide, 5x SSC pH 5 and 1% SDS in double-distilled water. After, they were washed three times for 20 minutes at 65°C with a solution of 50% formamide and 2x SSC pH 5 in double distilled water. Tris buffered saline solution plus Tween-20 (TBST) was used with the addition of 2mM of levamisole to wash the samples three times 10 minutes at room temperature. TBST consists of 140 mM of NaCl, 3 mM of KCl, 3 mM of Tris-HCl pH 7.5 and 0.1% of Tween-20. The samples were incubated in a blocking solution of 10% normal sheep serum in TBST for one to two hours at room temperature. During this time, the antibody mix was prepared. 0.0375 g of chick embryo powder was incubated in 6.25 ml of TBST for 30 minutes at 65°C. The solution was then put on ice. 62.5 µl of normal sheep serum and a 1:2000 dilution of α digoxigenin antibody were added to the chick embryo powder and TBST solution. It was put to rock at 4°C for an hour. The solution was then centrifuged at 13,000 rpm at 4°C for 10 minutes and the supernatant was transferred into another tube. The antibody mix was completed by adding 18.75 ml of TBST and 187.5 µl of normal sheep serum to the supernatant. The blocking solution was removed from the samples and replaced by antibody mix. They were

left rocking at 4°C overnight. The samples were washed three times for five minutes in TBST plus 2 mM of levamisole at room temperature. The levamisole must be added right before the first wash. Using fresh TBST plus levamisole solution, the samples were washed five times for an hour at room temperature. After, they were washed three times 10 minutes in NTMT (0.1 M NaCl, 0.1 M Tris-HCl pH 7.5, 50 mM MgCl₂ and 0.1% Tween-20). Coloring was performed by putting 2.5 µl of bromo-chloro-indolyl-phosphate (BCIP) and 2.5 µl of nitro blue tetrazolium (NBT) in 1 ml of NTMT. This solution was put on the samples and they were left soaking until specific purple staining was observed. The lungs were then photographed using the Zeiss SteREO Discovery.V8 microscope.

cDNA insert	Plasmid vector	Restriction enzyme	RNA Polymerase
Chick <i>Claudin-1</i>	pBluescript KS	NotI	T3
Chick <i>Claudin-3</i>	pBluescript KS	XhoI	T7
Chick <i>Claudin-4</i>	pCanHA3	BamHI	Sp6
Chick <i>Claudin-5</i>	pSC-A vector	XbaI	T3
Chick <i>Claudin-8</i>	pSC-A vector	BamHI	T3
Chick <i>Claudin-10</i>	pSC-A vector	BamHI	T3
Chick <i>Claudin-14</i>	pSC-A vector	BamHI	T3

Table 1. Restriction enzyme and RNA polymerase for the generation of chick *Claudin* antisense riboprobes.

2.3 Paraffin sections

The chick lung samples that were colored using *in situ* hybridization were washed three times in PBT for 10 minutes. They were then put in several washes of incremental concentration of ethanol in PBS (50%, 75%, 95%, 100%) for 30 minutes. They were washed a second time in 100% ethanol and put in xylene for two washes of 30 minutes. The samples were put in plastic molds and were covered with melted paraffin. They were then put in an airtight oven linked to a vacuum pump which was turned on for an hour to have an internal pressure of 15 kPa. After, the paraffin-embedded tissues were transferred to another plastic mold and were covered with fresh melted paraffin. They were put in the desired orientation (frontal or transverse). The molds were left at room temperature until the paraffin was completely solidified. The blocks were taken out of the mold and the base of the block was melted on a hotplate and mounted on a microtome plastic cassette. A sheet of aluminum foil was folded around the cassette to form a small recipient where melted paraffin was poured to fix the paraffin block to the cassette. The cassette was left at room

temperature until the paraffin was completely solid. The cassette was then mounted on the microtome by removing the aluminum foil and the excess of paraffin. The samples were sectioned at 7 μm for the samples placed in a transverse orientation and 10 μm for samples placed in a frontal orientation. The sections were then put in a 40°C water bath so they can spread out and mounted on Fisherbrand Superfrost Plus microscope slides. The slides were left on a slide warmer overnight. The slides are then washed two times for five minutes in xylene. The slides are then quickly dried. A drop of Permount is added on the slides and they are quickly covered with a glass coverslip. The sections were imaged using the Leica DFC450 C camera.

2.4 Cryosections

Collected chick lung samples were fixed 12 minutes at 4°C in a solution of 10% trichloroacetic acid (TCA) in PBS. They were then washed in a solution of 15% sucrose in PBS for an hour at room temperature (RT) and in a solution of 30% sucrose in PBS overnight at 4°C. After, they were washed an hour at room temperature in a solution of optimal cutting temperature (OCT) compound and 30% sucrose in PBS at a ratio of 1:1. The lungs were then placed at the bottom of a plastic mold and were covered with OCT compound. The samples were placed in the desired orientation. The molds were put in a bath of 100% ethanol with dry ice until the OCT compound was completely frozen. The blocks were stored at -80°C until they were sectioned with a cryostat microtome. Sections of different thickness were used. Transverse sections had a thickness of 10 μm and frontal sections had a thickness of 7 μm .

2.5 Immunofluorescence on cryosections

Immunofluorescence were performed on frontal and transverse lung cryosections. Transverse cryosections were obtained by sectioning along the length of the lung, from the most distal part to the trachea. Chick lung cryosections were blocked an hour at room temperature with 10% normal goat serum (NGS) in PBS containing 0.3% triton. The sections that were stained with Claudin-14 antibody were blocked using 10% bovine serum albumin (BSA) in PBS containing 0.3% triton. After, they were stained overnight at 4°C with a combination of different primary

antibodies with 5% NGS in PBS containing 0.3% triton: ZO-1 (Invitrogen, mouse α ZO1, 1:100), Claudin-3 (Abcam, Rabbit α Claudin-3, 1:100), Claudin-4 (Invitrogen, rabbit α Claudin-4, 1:100), Claudin-5 (Spring, Rabbit α Claudin-5, 1:100), Claudin-8 (Invitrogen, rabbit α Claudin-8, 1:100), Claudin-10 (Invitrogen, Rabbit α Claudin-10, 1:100), Claudin-14 (Sigma, goat α Claudin-14, 1:100), CPE (AbD Serotec, rabbit α CPE, 1:100). The sections were washed with PBS and stained with secondary antibodies in PBS containing 0.3% triton: Alexa Fluor 488 (Invitrogen, goat α rabbit or rabbit α goat, 1:500), Alexa Fluor 555 (Invitrogen, goat α mouse, 1:500), Alexa Fluor 647 (Invitrogen, goat α mouse, 1:500). The sections were coverslipped with SlowFade™ Gold Antifade Mountant with DAPI and put at 4°C. They were then imaged using the Zeiss LSM880 Laser Scanning Confocal microscope.

2.6 GST-C-CPE and GST protein production

Plasmid pET-14b containing the GST or GST-C-CPE construct were thawed on ice. We transform these plasmids into *E. coli* cells of the BL21 strain. An eppendorf of the BL21 competent cells were also thawed on ice. The cells were resuspended by gentle flicking. 45 μ l of cells were combined with 100 ng of plasmid in a 15 ml snap cap tube and this was put on ice for 30 minutes. A heat shock was then administered to the cells to create pores that will allow the plasmids to enter the cytoplasm. This was done by putting the eppendorf in a 42°C water bath for 45 seconds. The tube was then put back on ice for two minutes. 250 μ l of warm LB media was added and the tube was put in a shaker at 37°C with a speed of 250 rotations per minute (rpm) for an hour to an hour and a half.

During this time, a bottle of premixed LB media with agar-agar was put in the microwave at med-low power until the agar was completely melted. The bottle was then left unattended until its temperature was cold enough to be manipulated again. Ampicillin and chloramphenicol was then added to the solution at a concentration of 50 μ g/ml and 34 μ g/ml respectively. The bottle was shook and the LB-agar was poured in petri dishes. Around 15-20 ml of LB-agar was put per petri dish. The dishes were left at room temperature until they solidified. Using a Bunsen burner to create an aseptic environment, 30 and 75 μ l of the transformed cells were added to two LB-agar plates. The cells were then spread across the plate using a glass pasteur pipette curved by the flame. The plates were left to dry for 15 minutes and then put upside down in an incubator at

37°C for 12-16 hours. After, the plate was taken out of the incubator and a colony was picked using a toothpick or a pipette tip. The tip was put in a snap cap tube containing 4 to 5 ml of LB media with 50 µg/ml of ampicillin and chloramphenicol. The tube was put in the shaker at 37°C with a speed of 250 rpm for 12 to 16 hours.

The content of the tube was put in a 2 liters flask containing 400 ml of LB, 50 µg/ml of ampicillin and 34 µg/ml of chloramphenicol. 1 ml of LB alone was kept as a blank control for spectrophotometry. The flask was put 2 hours in the shaker at 37°C with a speed of 250 rpm. The absorbance of the cultures was determined using spectrophotometry. 1 ml of media was put in a plastic cuvette. A photospectrometer was used to check the absorbance at a wavelength of 595 nm. If the absorbance was lower than 0.4, the flask was put back in the shaker for 15 minutes until the absorbance was 0.4 or higher. When the desired absorbance was reached, the content of the flask was induced by adding 0.1 mM of IPTG. The flask was put in the shaker for 12-16 hours at 20°C for the GST-CPE protein or 37°C for the GST protein. The cell culture was poured in two centrifuge cone tubes (200 ml each) and their weight were equalized using a balance. They were centrifuged at a speed of 4000 rpm and a temperature of 4°C for 15 minutes. The supernatant was removed and the precipitation was resuspended in 10-20 ml of LB. The content of both bottles were put in a 50 ml tube and it was centrifuged at 3000 rpm for 15 minutes at 4°C using a 50 ml tube filled with water to equalize. The tube was then stored in the -80°C freezer until purification.

To purify the proteins, the protein pellet was thawed in ice. During this time, the sodium chloride-tris-ethylenediaminetetraacetic acid (STE) buffer was made. STE buffer consists of 150 mM NaCl, 1 mM EDTA and 10 mM Tris-HCl pH 8 in double-distilled water. 50 ml of the STE buffer was taken and mixed with different protease inhibitors: aprotinin (1:10,000), leupeptin (1:10,000), pepstatin A (1:10,000) and phenylmethylsulfonyl fluoride (PMSF) (57 U/ml). 20 ml of buffer containing the protease inhibitors was added to the protein pellet and resuspended slowly with a plastic transfer pipette. Lysozyme (100 µg/ml) was added to the tube and it was left on ice for five minutes. The sample was then transferred to a small centrifuge tube and sonicated three times 30 seconds with a waiting time of a minute between each sonicating period. The samples were always kept on ice. To sterilize the sonicator, it was put in a solution of 75% ethanol and then put in water between every period of sonication. The tubes were balanced and centrifuged for 15 minutes at 15,000 rpm. Next, the supernatant was put in a 50 ml tube. The purification beads were prepared by

taking 200 μ l of 50% slurry (a mixture of beads and 80% ethanol) and washing them three times in STE buffer. Before removing the last STE wash, the mixture was centrifuged at 500 rpm for a minute. The STE was replaced by fresh STE until it reached a volume of 1 ml and the beads were resuspended gently. They were added to the tube containing the supernatant. It was then left rocking at 4°C overnight with parafilm around the cap to avoid leaks. The tube was then balanced and centrifuged for five minutes at 500 rpm. 15 ml of the supernatant was taken out and kept in a 15 ml tube labeled as unbound product. The rest of the supernatant was disposed. STE was added to the beads until it reached 10 ml and was transferred to a 15 ml tube. The previous 50 ml tubes were kept. The beads were incubated in ice for 10 minutes. During this time, the glutathion stock and the elution buffer was prepared. The tube with beads was balanced and centrifuged for 5 minutes at 500 rpm. The supernatant was discarded. 5 ml of STE was added in the previous 50 ml tube to collect the leftover beads on the tube wall and was then added to the 15 ml tube containing the beads. This tube was then balanced and centrifuge again at 500 rpm for 5 minutes. The high and low pH buffers were prepared. The supernatant was discarded. 10 eppendorf tubes were labeled as E1 to E10. A purification column was prepared by breaking the tip and by pipetting STE buffer in it until liquid was dropping from the bottom of the column. The column was put in a clean eppendorf and the samples containing the beads were put drop by drop in the column. The tube that was containing the beads was washed with STE to retrieve the rest of the beads and they were transferred to the column. The beads were washed 3 times with STE by letting it fully flow out of the columns. Elution buffer was added to the beads and was left incubating at room temperature for 1 hour with the cap on the column. The column was then put in the E1 eppendorf tube and the drops were collected by changing eppendorf tube whenever a volume of 500 μ l was reached. To check if the eluted product contained proteins, a Bradford assay was done. 1 ml of Bradford reagent solution (1:5 dilution in double-distilled water) was put in a photospectrometry cuvette and 1 μ l of sample was added and mixed by swirling gently the cuvette. This was done for the first 5 eppendorfs (E1 to E5). If no protein was detected by seeing a change of color from brown to blue, the other 5 eppendorfs were assayed. Absorbance was then measured using a spectrophotometer at a wavelength of 595 nm. The eppendorfs which had an absorbance measure higher than 0.2 were mixed together. 6 liters of PBS were prepared and put at 4°C until cold. A dialysis cassette (Qiagen) was put in a foam holder and in the cold PBS for 3 minutes. With a syringe, the protein product transferred from the eppendorf to the cassette by making sure that no air was left in the cassette. It was then put in the cold PBS with a magnetic

stirrer and left overnight. The PBS was replaced by fresh PBS after 2 hours and the next morning. The product was collected with a syringe and aliquoted in eppendorf tubes. These were stored at -80°C . A Bradford assay was performed to determine protein concentration and it was confirmed by running a certain volume of the protein solution with different volumes of BSA solution with a known concentration. To restore beads, they were washed three times with high and low pH buffers consecutively, wash in PBS and store in a solution of 70% ethanol in PBS. High and low pH buffers consist of 0.1 M Tris-HCl and 0.5 M NaCl with an adjusted pH of 8.5 and 4.5 respectively.

2.7 Chick and mouse embryonic lung explants culture

E5 chick lungs and E12.5 mouse lungs were dissected and put on a track-etched polyethylene terephthalate membrane (Corning™ Falcon™ Cell Culture Inserts) in a 6-well plate. DMEM/F12 media was added in the well with 1% streptomycin and penicillin and 10% fetal bovine serum (FBS) for the mouse lungs or 5% FBS and 5% chicken serum for the chick lungs. Treatments were administered to the lung by adding PBS (no treatment) or different concentrations of GST or GST-C-CPE directly to the media. We are using a C-CPE protein fused with a GST tag for purification purposes. To ensure that the effects seen in the GST-C-CPE treated samples are attributed to C-CPE, we perform a second control group which is treated with GST-only at the same molarity as the GST-C-CPE treated group.

The plate was put in a humidified incubator with 5% CO_2 and 10% O_2 . The lungs were cultured for up to 72 hours and the culture dish was removed from the incubator to take pictures at time 0 and every 24 hours.

2.8 Chick lung measurements

The airway perimeter was measured by outlining the epithelial cells of the airway structures every 24 hours using ImageJ. Using the perimeter and ImageJ, the lumen area was also measured. This was done 3 times per picture and an average of the 3 areas was kept. This was measured blindly. The buds were also counted every 24 hours, and this was also done blindly.

2.9 Statistical analyses

To determine significance, statistical analyses were performed on the chick lung measurements. Graphs and statistical tests were done using GraphPad Prism. The Shapiro-Wilk test was used to test normality of the measurements. To determine if two groups are significantly different from each other, one-way ANOVA with Tukey's Multiple Comparison test was used. The data was presented with the standard deviation from the mean and significance level of 0.05 was used.

2.10 Whole mount immunofluorescence

Mouse lungs were removed from the membrane after culture and fixed for 12 minutes at 4°C with 10% TCA in PBS. They were washed three times for five minutes in PBS and then blocked for an hour at room temperature with 10% NGS in PBS containing 0.3% triton. They were stained overnight at 4°C with a combination of different primary antibodies with 5% NGS in PBS containing 0.3% triton: ZO-1 (Invitrogen, mouse α ZO1, 1:100) and Claudin-3 (Spring, Rabbit α Cldn3, 1:100). They were washed with PBS and stained with secondary antibodies in PBS containing 0.3% triton: Alexa Fluor 488 (Invitrogen, goat α rabbit, 1:500), Alexa Fluor 555 (Invitrogen, goat α mouse, 1:500). The explants were put in SlowFade™ Gold Antifade Mountant with DAPI (Invitrogen) overnight at 4°C. They were then fixed 12 minutes in 4% PFA at 4°C and washed for 30 minutes in a solution of methanol and PBS at increasing concentration (50%, 75%, 95%, 100%). The lungs were placed on a slide surrounded by a Secure-Seal™ Spacer (one well, 13 mm diameter, 0.12 mm deep; Invitrogen™). A drop of a solution of benzyl alcohol and benzyl benzoate (2:1) was put on the lungs. They were then coverslipped and stored at 4°C. Pictures were taken using the Zeiss LSM880 Laser Scanning Confocal microscope.

CHAPTER 3: Results

3.1 Analysis of claudin expression during chick lung branching morphogenesis

Previous studies from my lab looked at claudin expression patterns during chick embryogenesis. Data from RT-PCR and *in situ* hybridization analyses showed that *Claudin-1*, *Claudin-3* and *Claudin-10* mRNA are expressed in chick lungs during early development (Simard *et al.*, 2005, Collins *et al.*, 2013). However, the focus of these experiments was not lung development and, consequently, important timepoints during chick lung branching were not considered and *in situ* hybridization was only performed on whole embryos, which can limit the resolution of detection. In the paper by Collins *et al.* (2013), claudin mRNA expression, with the exception of *Claudin-1* and *-5* was studied in the lung at E5, E7 and E10. No complete expression of the first stages of the chick lung branching morphogenesis was done. Also, in these previous studies, protein expression was not assayed, which is necessary to show that not only is the mRNA is synthesized, but the protein is also produced. Therefore, to fully characterize claudin mRNA and protein expression during early chick lung branching morphogenesis, I used *in situ* hybridization and immunofluorescence analyses to examine expression of *Claudin-3*, *-4*, *-8* and *-14*, which are sensitive to C-CPE. In addition, I examined *Claudin-1* and *-10* mRNA expression, which are expressed during the development of the kidney, another branched organ. *Claudin-5* expression was also examined because it has been shown to be located in the chick embryo vasculature (Collins *et al.*, 2012). mRNA and protein expression were analyzed at E4, E5 and E6. The first buds appear between E4 and E5 and they branch and expand between E5 and E6. E5 is also the stage when lung explants will be treated with C-CPE for Objective 2. *In situ* hybridization was performed on whole mount embryonic chick lungs, which were then embedded in paraffin and sectioned. Immunofluorescence of *Claudin-1*, *-3*, *-4*, *-5*, *-8*, *-10* and *-14* was performed on transverse cryosections.

3.1.1 Claudin mRNA expression

In E4 chick lungs, *Claudin-1* mRNA was expressed in the epithelial cells along the trachea and the bronchi (Figure 5 A). At E5 and E6, it was expressed along the epithelial cells of the trachea, the primary bronchi and the secondary bronchi buds. (Figure 5 B, B' and C).

Like *Claudin-1*, *Claudin-3* mRNA was observed in the epithelial cells along the trachea and the bronchi of E4 lung (Figure 5 D). At E5 and E6, it was expressed along the epithelial cells of the

trachea, the primary bronchi and the secondary bronchi buds. In E6 lungs, expression appeared to be highest in the secondary bronchi buds (Figure 5 E, E' and F).

Claudin-4 mRNA expression was seen in some epithelial cells of E4 (Figure 5 G and G') and E5 lungs (Figure 5 H and H'). In E6 lungs, staining was also seen (Figure 5 I and I'), but the majority of this staining appeared to be caused by trapping (Figure 5 I', red arrowhead) and edge effect (Figure 5 I', black arrowhead). When *in situ* hybridization using a sense probe was performed, a similar staining pattern was observed in chick lungs. This means that the *Cldn4* mRNA expression pattern observed in this experiment may not be specific (Figure 5 V and V').

Claudin-5 mRNA was not expressed in the epithelial cells of E4, E5 and E6 chick lungs (Figure 5 J, K, K' and L). However, *Claudin-5* mRNA was expressed in the endothelial cells of the blood vessels at E4, E5 and E6. (Figure 5 K').

Claudin-8 mRNA was not observed in the buds or in the epithelial cells in any studied stage (Figure 5 M, N, N' and O).

Claudin-10 mRNA was expressed throughout the epithelial cells of the trachea and the bronchi in E4 lungs. At E5 and E6 lungs, it was expressed in the epithelial cells of the trachea, the bronchi and the buds (Figure 5 P, Q, Q' and R).

Claudin-14 mRNA was not expressed in E4 lungs (Figure 5 S, T, U and U'). Whole mount *in situ* shows staining in E5 and E6 lungs. However, after sectioning, the staining was revealed to be different than the cytoplasmic staining seen in samples stained with *Claudin-1*, -3 and -10 probes. Staining was seen inside the lumen and at the apical side of the epithelial cells suggesting that it was caused by trapping and edge effects.

Claudin-1, -3 and -10 mRNA expression were observed in the esophagus (Figure 5 A, B, C, F, P, Q and R). This is interesting because like the lungs, the esophagus derives from the primitive gut, at the foregut domain.

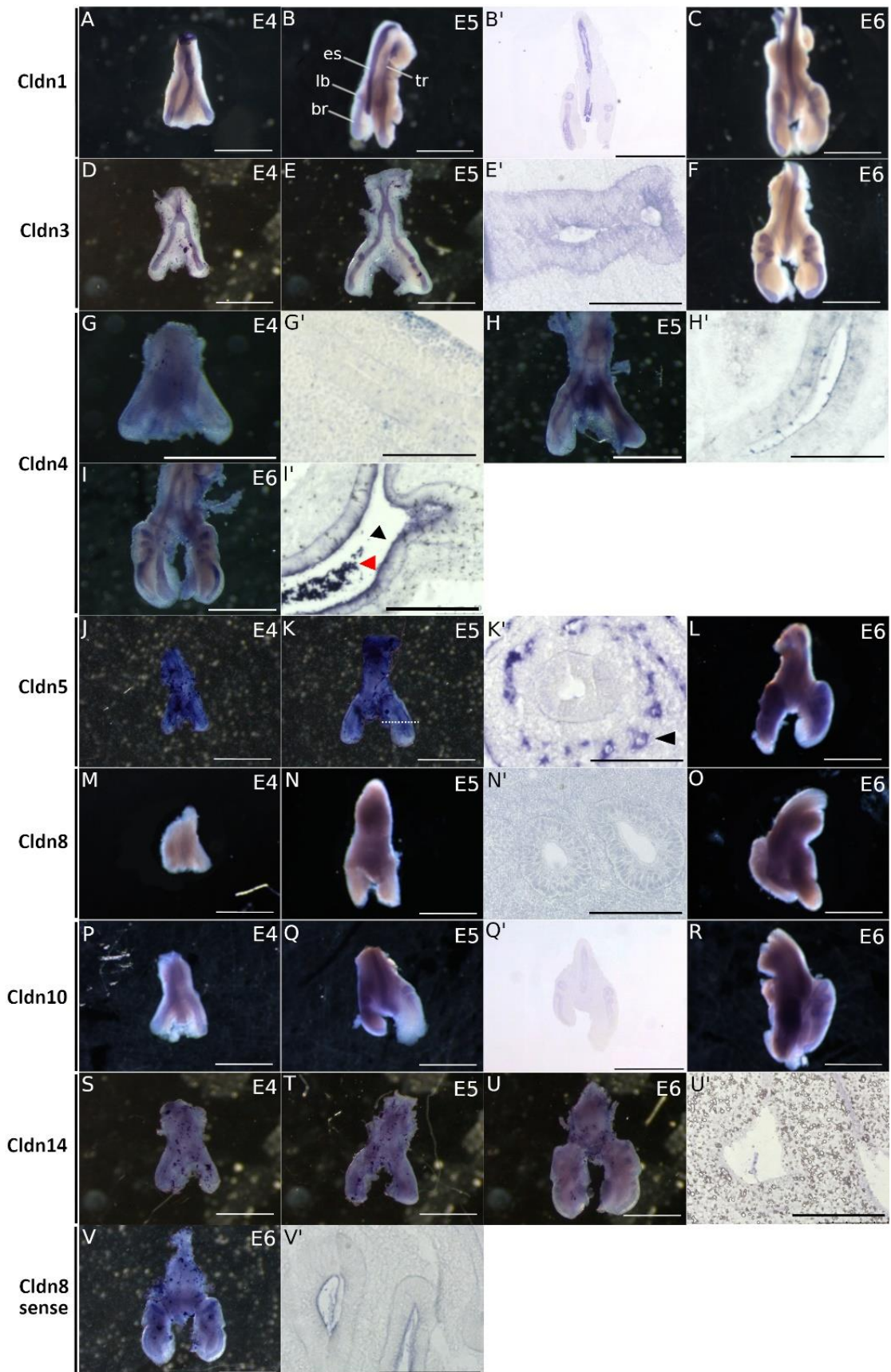


Figure 5. Analysis of *Claudin* expression in E4-E6 chick lungs.

Whole mount *in situ* hybridization method was used to assess expression of *Claudin-1* (A-C), -3 (D-F), -4 (G-I), -5 (J-L), -8 (M-O), -10 (P-R) and -14 in E4, E5 and E6 chick lungs. Frontal sections were obtained for samples B, E, G, H, I, N, Q and U (B', E', G', H', I', N', Q' and U'). Transverse section at the dotted line of sample K was obtained (K'). Whole mount *in situ* hybridization was also performed using a *Cldn8* sense probe to test specificity (V) Frontal sections were also obtained (V'). Abbreviations: es, esophagus; lb, lung bud; br, bronchi; tr, trachea. Scale bars : A-U, 1 mm; E', G', H', I', K', N' and U', 100 μ m; B' and Q', 750 μ m.

3.1.2 Claudin protein expression

Similar to the mRNA expression, Claudin-1 protein is expressed at the apical surface of all E4 lung epithelial cells including the bronchi and the trachea. It is also colocalized with ZO-1 (Figure 6). In E5 lungs, Claudin-1 was expressed on the apical side of all the epithelial cells of the primary bronchi and the trachea but not in the cells of the secondary bronchi bud. (Figure 6). In E6 lungs, Claudin-1 protein was observed on the apical surface of epithelial cells, but it had a more punctate pattern of expression than in E4 and E5 and it was not seen in the cells of the secondary structures that branch from the primary bronchi. However, this diffuse weak staining may not be specific. Similar diffuse expression was seen in the negative control, which was secondary antibody alone (Figure 9).

At the E4 timepoint, Claudin-3 protein expression corresponded to its mRNA expression. It was expressed at the apical surface of the epithelial cells of the bronchi and the trachea colocalizing with ZO-1 (Figure 6). In E5 lungs, protein expression was also seen at the apical surface of all epithelial cells, but it had a more punctate pattern. Contrary to Claudin-1 expression, there was no difference in expression between primary bronchi and secondary bronchi buds. In E6 lungs, the Claudin-3 protein expression pattern was similar to E5 lungs and, in contradiction to what was seen in *Claudin-3* mRNA expression, there was no obvious expression difference between the primary bronchi and the secondary structures (Figure 6).

Although I observed a limited amount *Claudin-4* mRNA expression, immunofluorescence analysis of E4 lungs revealed Claudin-4 protein expression on the apical side of all epithelial cells colocalizing with ZO-1. In E5 and E6, its expression was more diffused with less clear staining observed. Less colocalization with ZO-1 was observed (Figure 7). This staining may not be specific based on the diffuse weak signal seen also in the no primary antibody control (Figure 9). Protein

expression in E5 and E6 corresponds to mRNA data that showed *Claudin-4* mRNA expression in some epithelial cells.

Contrary to the mRNA, Claudin-5 protein was expressed in the epithelial structures. In E4 lungs, Claudin-5 protein was expressed at the apical surface of the epithelial cells of the bronchi and the trachea colocalizing with ZO-1 (Figure 7). In E5 lungs, protein expression was also seen at the apical side of epithelial cells, but like Claudin-1, expression was stronger in primary bronchi than in secondary bronchi buds. This was also observed in E6 lungs where Claudin-5 protein was expressed at the apical side of every epithelial cells, but its expression appeared stronger in primary bronchi than in secondary structures (Figure 7). Claudin-5 expression was also observed in endothelial cells of the blood vessels surrounding the epithelial structures in all studied stages. E6 lungs showed less endothelial structures than in E4 and E5. (Figure 10, red arrowheads).

Like its mRNA expression, Claudin-8 protein was not detected in the lung epithelial cells at E4 (Figure 8). Faint expression was detected in E5 and E6 lungs, but similar signal was also seen in the no primary antibody control suggesting the signal is not specific for Claudin-8 (Figure 9).

Correlating with its mRNA expression, Claudin-10 protein was expressed on the apical side of the epithelial cells in the bronchi, the secondary buds and the trachea of E4 lungs (Figure 8). The expression pattern is punctate, following ZO-1 expression only at specific places. In E5 lungs, Claudin-10 protein expression was seen colocalizing with ZO-1. In E6 lungs, faint expression was observed at the apical side of epithelial cells (Figure 8).

Contrary to mRNA expression, Claudin-14 immunofluorescence showed protein expression at the apical side of all epithelial cells in E5 chick lungs colocalizing with ZO-1. Claudin-14 immunofluorescence in E5 lungs showed stronger staining in the primary bronchi than in the secondary bronchi buds. In E6 lungs, really faint Claudin-14 protein expression was observed at the apical side of epithelial cells (Figure 9).

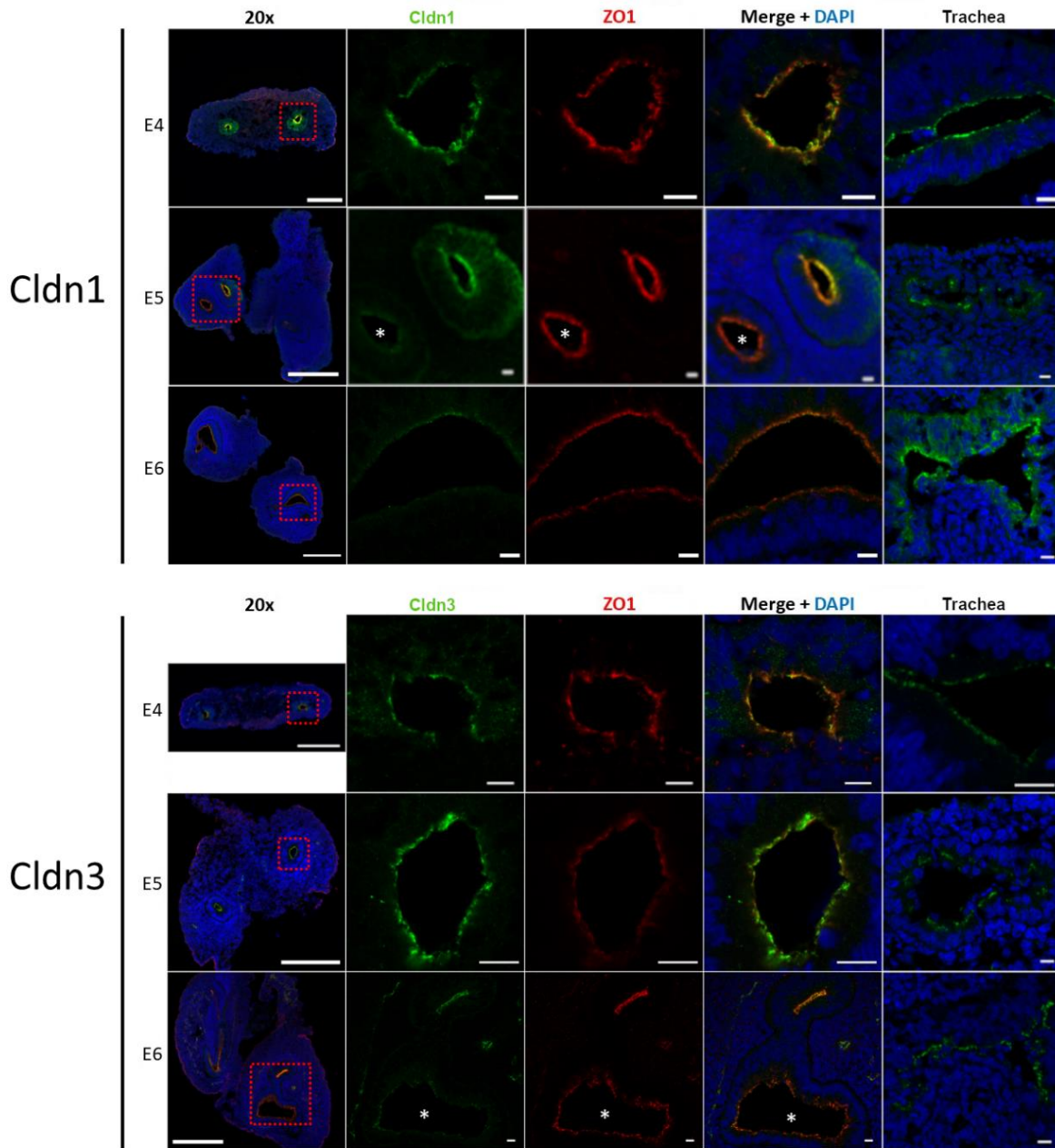


Figure 6. Characterization of Claudin-1 and -3 expression in branching chick lungs.

Immunofluorescence targeting Claudin-1 and -3 (green) and ZO-1 (red) was performed on 10 μm cryosections of E4, E5 and E6 chick lungs and tracheas. These sections were imaged using a confocal microscope. Scale bars: 200 μm in the 20x column and 10 μm in the other columns. Asterisk: secondary bronchi.

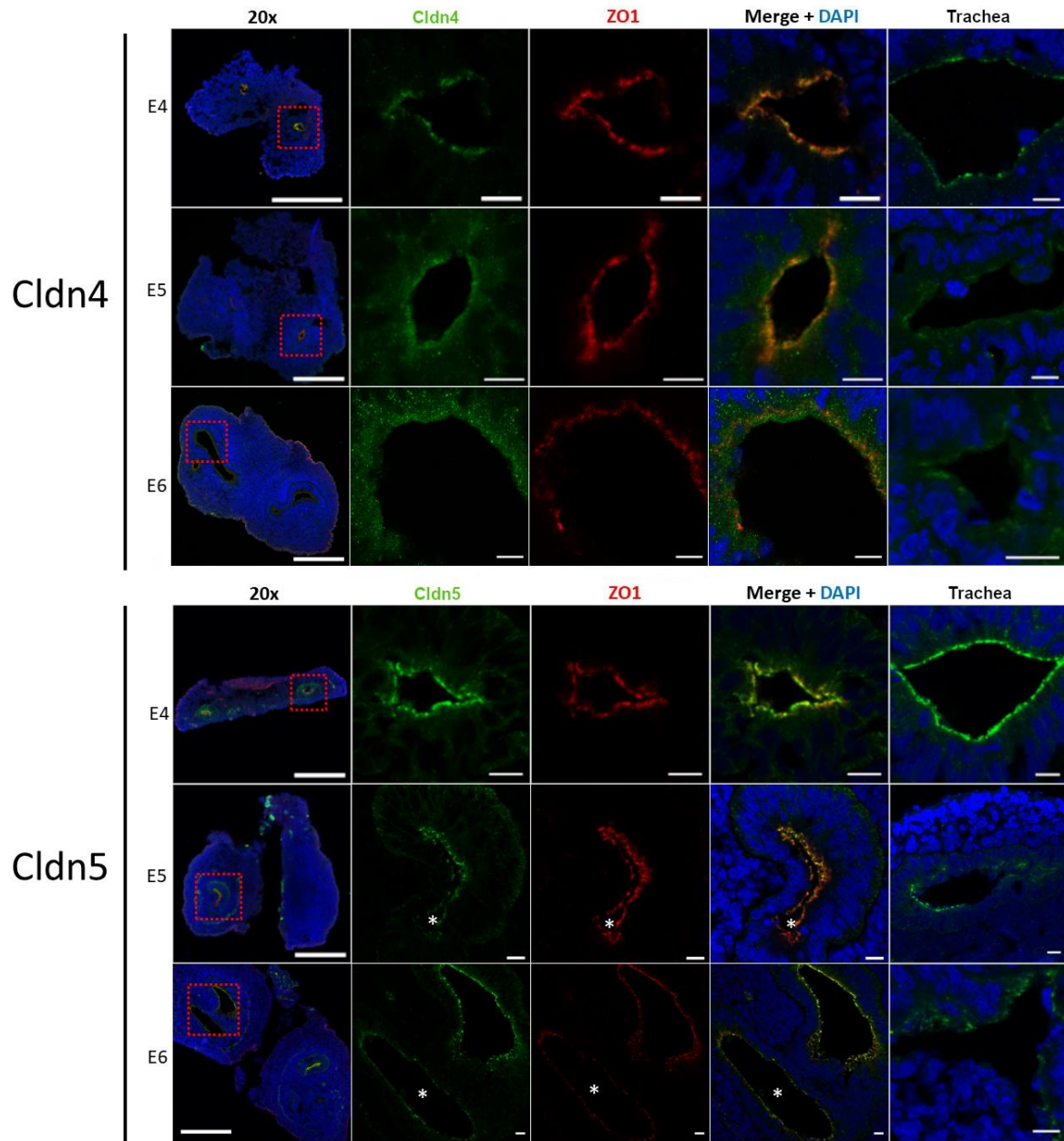


Figure 7. Characterization of Claudin-4 and-5 expression in branching chick lungs.

Immunofluorescence targeting Claudin-5, -8 and -10 (green) and ZO-1 (red) was performed on 10 μm cryosections of E4, E5 and E6 chick lungs and tracheas. These sections were imaged using a confocal microscope. Scale bars: 200 μm in the 20x column and 10 μm in the other columns. Asterisk: secondary bronchi.

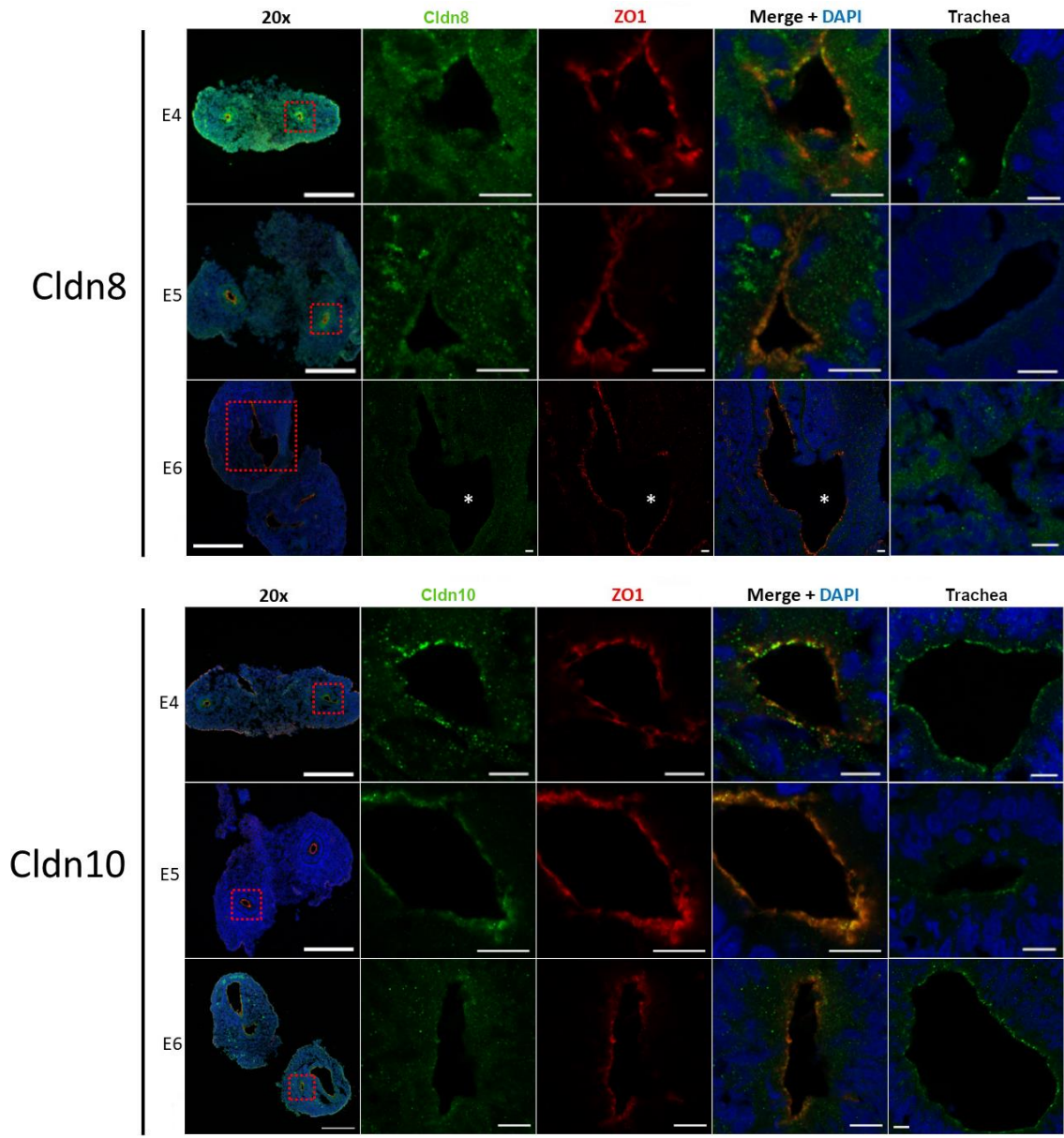


Figure 8. Characterization of Claudin-8 and -10 expression in branching chick lungs. Immunofluorescence targeting Claudin-5, -8 and -10 (green) and ZO-1 (red) was performed on 10 μm cryosections of E4, E5 and E6 chick lungs and tracheas. These sections were imaged using a confocal microscope. Scale bars: 200 μm in the 20x column and 10 μm in the other columns. Asterisk: secondary bronchi.

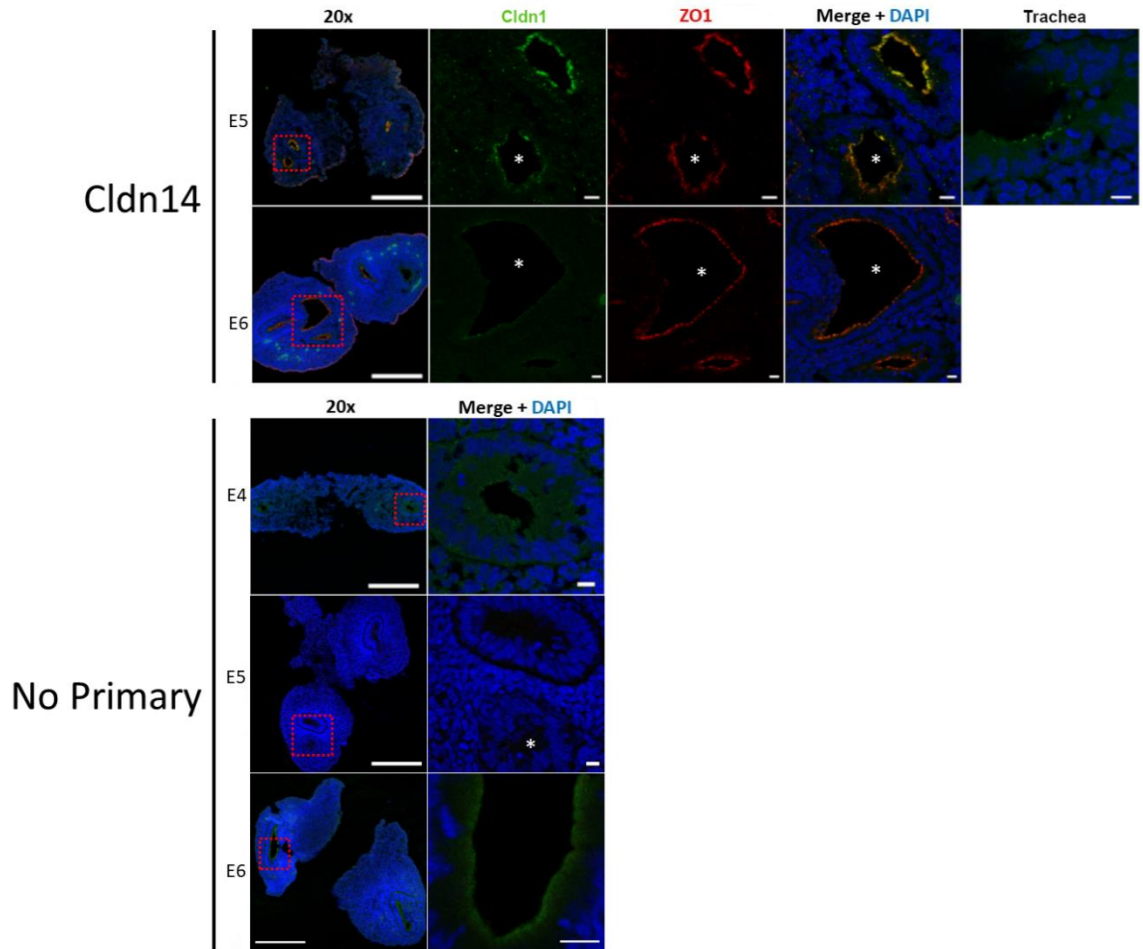


Figure 9. Characterization of Claudin-14 in branching chick lungs and no primary control. Immunofluorescence targeting Claudin-14 (green) and ZO-1 (red) was performed on 10 μm cryosections of E5 and E6 chick lungs, and E5 tracheas. No primary control was also done on 10 μm cryosections of E4, E5 and E6 chick lungs. Sections were imaged using a confocal microscope. Scale bars: 200 μm in the 20x column and 10 μm in the other columns. Asterisk: secondary bronchi.

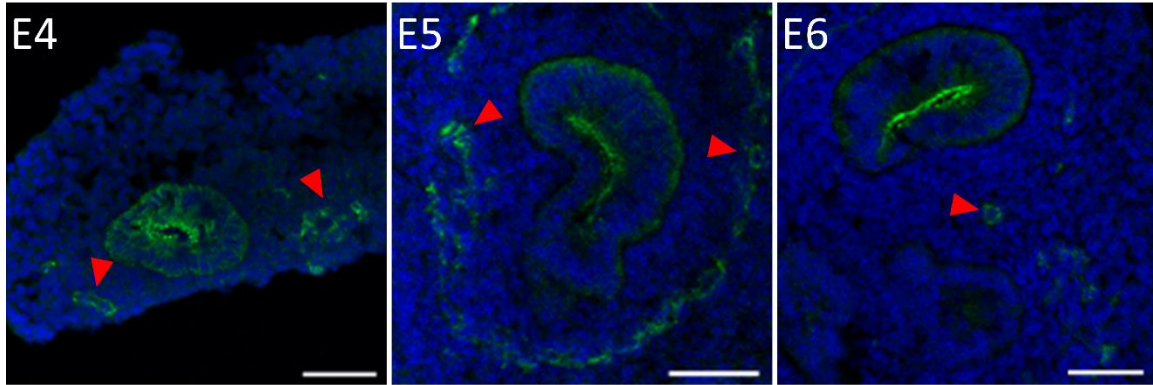


Figure 10. Characterization of Claudin-5 expression in epithelial and endothelial cells of branching chick lungs.

Immunofluorescence targeting Claudin-5 (green) was performed on 10 μm cryosections of E4, E5 and E6 chick lungs. Expression was observed in epithelial and endothelial cells (red arrowheads) of E4, E5 and E6 chick lungs. Less structures were seen in E6 chick lungs. Scale bars: 50 μm .

Claudins	mRNA expression			Protein expression		
	E4	E5	E6	E4	E5	E6
Cldn1	+	+	+	+	+	+
Cldn3	+	+	+	+	+	+
Cldn4	-	-	-	+	+	-
Cldn5	*	*	*	+	+	+
Cldn8	-	-	-	-	-	-
Cldn10	+	+	+	+	+	-
Cldn14	-	-	-	n/a	+	-

-, absent expression; +, positive expression; *, expression in endothelial cells; n/a, no data available yet.

Table 2. Summary of mRNA and protein expression for a subset of claudins in the chick lung at E4, E5 and E6.

3.2 Establishing conditions to grow embryonic chick lungs *ex vivo*.

To study the role of claudins in chick and mouse lung branching morphogenesis, we chose to use *ex vivo* lung explant culture for several reasons. This technique allows us to have total control on the culture conditions. We can determine the effect of changing a variable on the development of the organ. Also, *ex vivo* culture permits the monitoring of the organ continuously, enabling us to do live imaging and to study its development in detail. The culture of embryonic lung explants

gives the organ a more flattened appearance allowing us to see the formation of all the terminal branch points on the same focal plane making it easier to observe the phenotype. Many studies have been performed using lung explant culture. For example, FGF signaling during chick lung development was studied by inhibiting different pathway members in an *ex vivo* cultured embryonic lung (Moura *et al.*, 2011). Obviously, the main disadvantages of this method are that it can be used only for a limited time (up to 4-5 days) and the rate of development is greatly diminished. *In vivo* studies should also be used to complete and confirm the findings.

To study chick lung branching morphogenesis, the conditions for *ex vivo* culture of chick lungs were established. After reviewing the literature, we adapted an *ex vivo* protocol to culture kidney explants and applied this to chick lung explants. To have the optimal chick lung growth, different conditions and materials were tested. First, I compared two compositions of sera to culture embryonic chick lung explants: 10% fetal bovine serum or a mix of 5% fetal bovine serum and 5% chicken serum. The lungs cultured with these two conditions grew similarly (Figure 11). I chose to culture chick lungs with a combination of fetal bovine serum and chicken serum based on a paper by Moura *et al.* (2011).

Next, I determined which stage was the best to culture chick and mouse lungs and to study their branching patterns. For the culture experiments, I wanted to choose a stage that was not too early so that the lungs would grow and branch, but not so late that the explants were already very branched, which would make it more challenging to discern differences in branching patterns between controls and treated lungs. I compared the culture of E4 to E5 chick lungs, which are the two first days of the lung branching morphogenesis. E5 chick lung explants grew much better and formed more complex structures than E4 chick lung explants (Figure 12). I concluded that E5 was the most optimal timepoint to explant lungs into culture and observe branching patterns.

I also compared membrane inserts with two different pore sizes: 8 and 0.7 μm . I observed that chick lung explants cultured on a membrane insert with a pore size of 8 μm exhibited an improved growth when compared to chick lung explants cultured on 0.7 μm inserts (Figure 13).

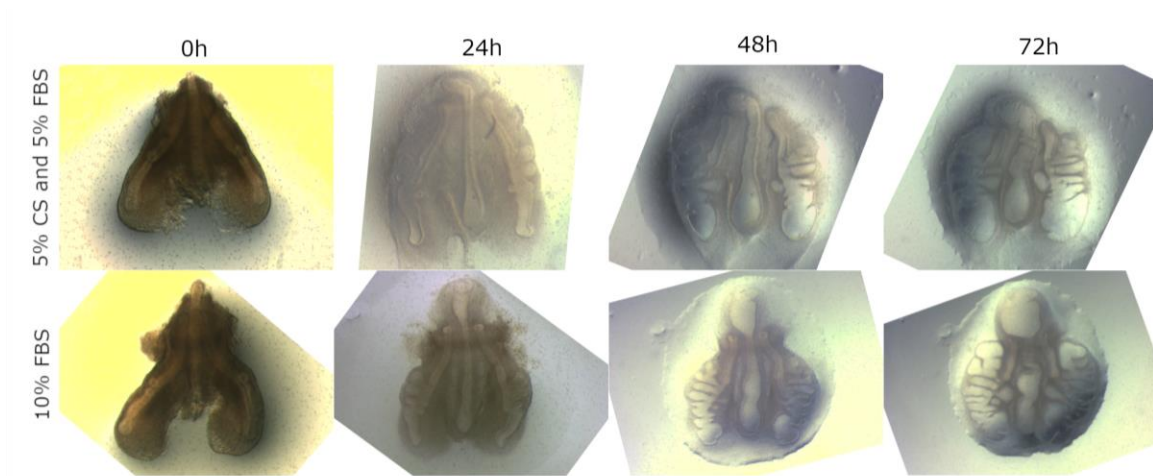


Figure 11. Chick lung explants cultured with 5% chicken serum and 5% FBS or 10% FBS grow similarly.

E5 chick lungs were cultured with 5 chicken serum (CS) and 5% fetal bovine serum (FBS) or with 10% FBS on 8 μ m pore filter for 72h. Pictures were taken every 24h.

To determine the optimal way to treat lung explants with C-CPE, different methods were tested. First, agarose beads soaked in GST or GST-C-CPE were put on the lung explants and these were cultured for 72h on an insert (Figure 14). The advantage of this technique was that the control could be done on the same lung, with one bronchi having a GST-soaked bead and the other a GST-C-CPE soaked bead. Unfortunately, the amount of C-CPE captured and released by the bead cannot be measured precisely and the physical presence of the bead can also affect branching by blocking the growth of the lung structures. The precision of the beads' position and the bead size were also factors. The control and the treated beads could not be placed exactly at the same position, making it hard to compare both sides. C-CPE injection was also tried in the lung explants through the trachea. This method was used because the reagent was certainly localized inside the explant's lumen, where it would target the claudins. Unfortunately, only a few had the C-CPE reaching all the bronchi. In the other explants, C-CPE would get stuck in the trachea or the needle would perforate the lumen. Because of the very low percentage of C-CPE-injected explants, adding C-CPE directly in the media was used in the subsequent experiments.

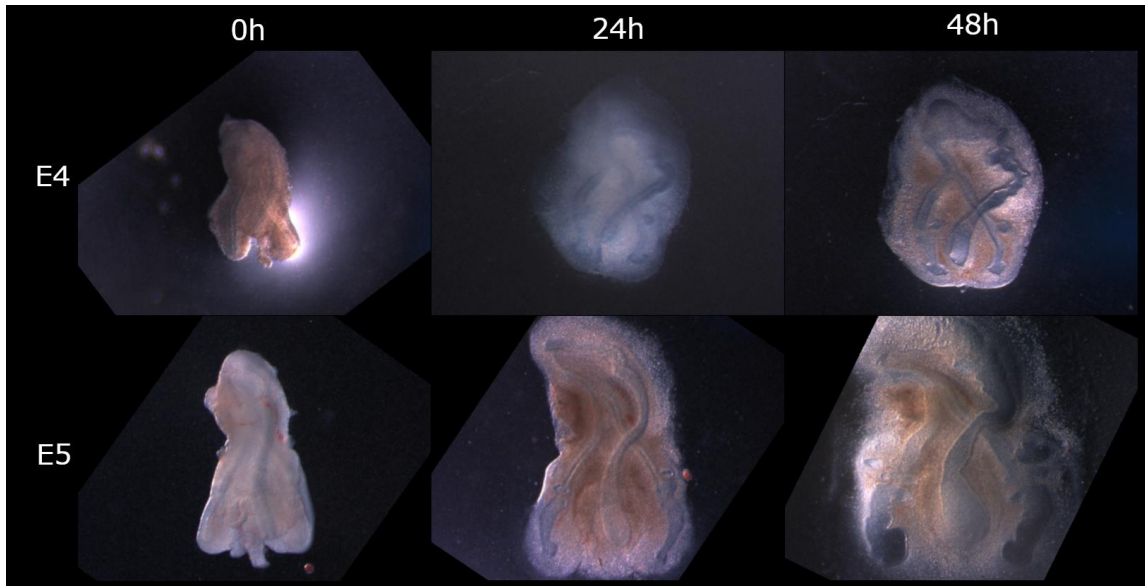


Figure 12. Cultured E5 chick lung explants have a more complex structure than E4 lungs. E4 and E5 chick lungs were cultured simultaneously on 8 μm pore filter for 48 hours. Pictures were taken every 24 hours.

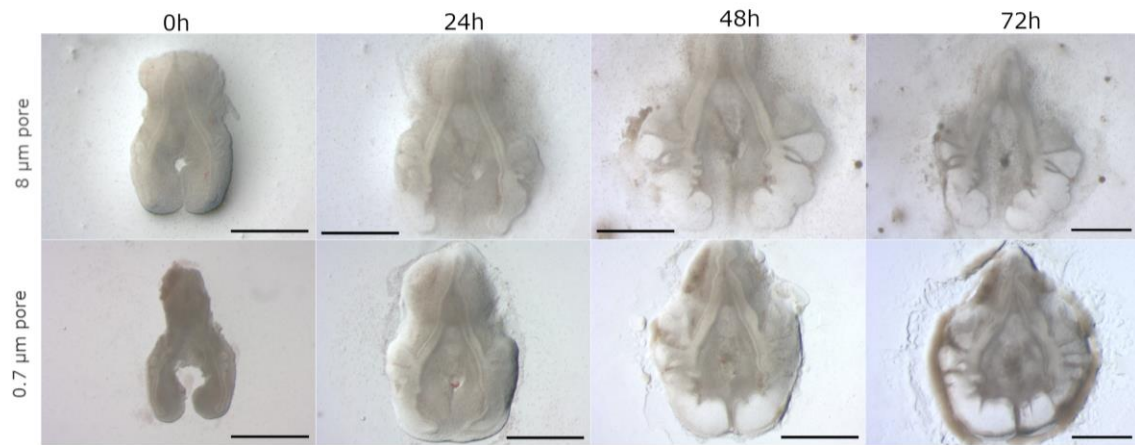


Figure 13. Chick lung explants exhibited improved growth when cultured on inserts with 8 μm pore filters than on those with 0.7 μm pores. E5 chick lungs were grown on 8 μm or 0.7 μm pore filters for 72 hours. Pictures were taken every 24 hours. Scale bars: 1 mm.

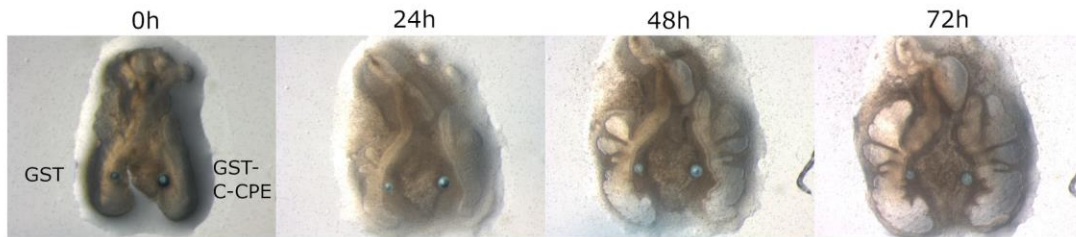


Figure 14. C-CPE-soaked beads do not affect primary branching in explant cultures of chick lungs.

GST and GST-C-CPE-soaked beads were placed on E5 chick lung and cultured 72h on 8 μm pore filters. GST-soaked beads were positioned on the left bronchi while GST-C-CPE-soaked beads were on the right bronchi. Pictures were taken every 24 hours.

To improve the relevance of the comparison between C-CPE-treated explants and controls, other ways to culture the lungs were tested. Lung explants were cut in half to have one bronchi cultured on media treated with GST and one bronchi cultured on media treated with GST-C-CPE. This would allow a more significant comparison between treated explants and controls. The half-lungs grew and branched, but there were differences between the two halves when cultured with the same non-treated media. For example, after 72 hours of culture the second most proximal bud of the second half explant is more developed than in the first half (Figure 15, black arrowheads). This difference suggested that it might not be a proper control. That is why whole lung explant culture was used in later experiments. Also, a previous study showed that cauterizing the trachea of mouse lung explants had an effect on branching (Unbekandt *et al.*, 2008). To determine if it would also have an effect on chick lung branching during the culture experiments, lung explants with cauterized trachea were cultured and compared with the non-cauterized explants. No strong evidence suggested a difference between cauterized and non-cauterized lung explants (Figure 16). Therefore, non-cauterized lungs were used in subsequent experiments to avoid additional disruptions to the growing lung explants.

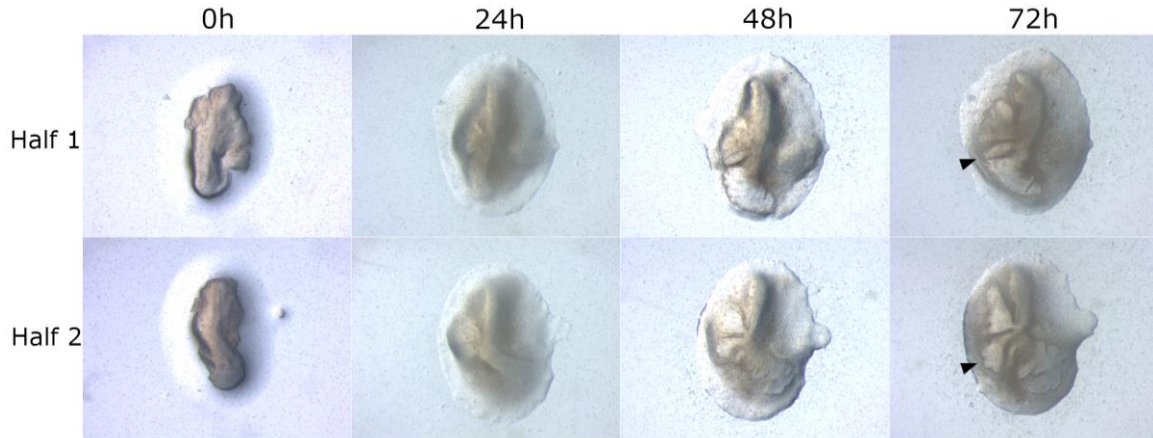


Figure 15. Bisected E5 chick lungs had distinct branching patterns in explant culture.
 Bisected E5 chick lungs were grown on 8 μm pore filters for 72 hours. Pictures were taken every 24 hours. Differences in development was observed between two halves of the same lung (black arrowheads).



Figure 16. Cauterizing E5 chick lungs did not affect development of the explant.
 E5 chick lungs were grown with a non-cauterized trachea or with a cauterized trachea on 8 μm pore filters for 72 hours. Pictures were taken every 24 hours.

In the mouse, I compared E11.5 and E12.5 lung explants and I observed that E12.5 lung explants branch a lot, suggesting that an earlier time point might be a more optimal stage for phenotype analysis. However, E11.5 lung explants did not branch sufficiently to allow me to properly characterize the differences between treatments (Figure 17). Also, there was more variability in the branching of E11.5 lung explants: some did not branch, and others had some branching. I

concluded that for embryonic mouse lung explants, E12.5 was the optimal stage for my experiments because they branched more and had less variability between explants.

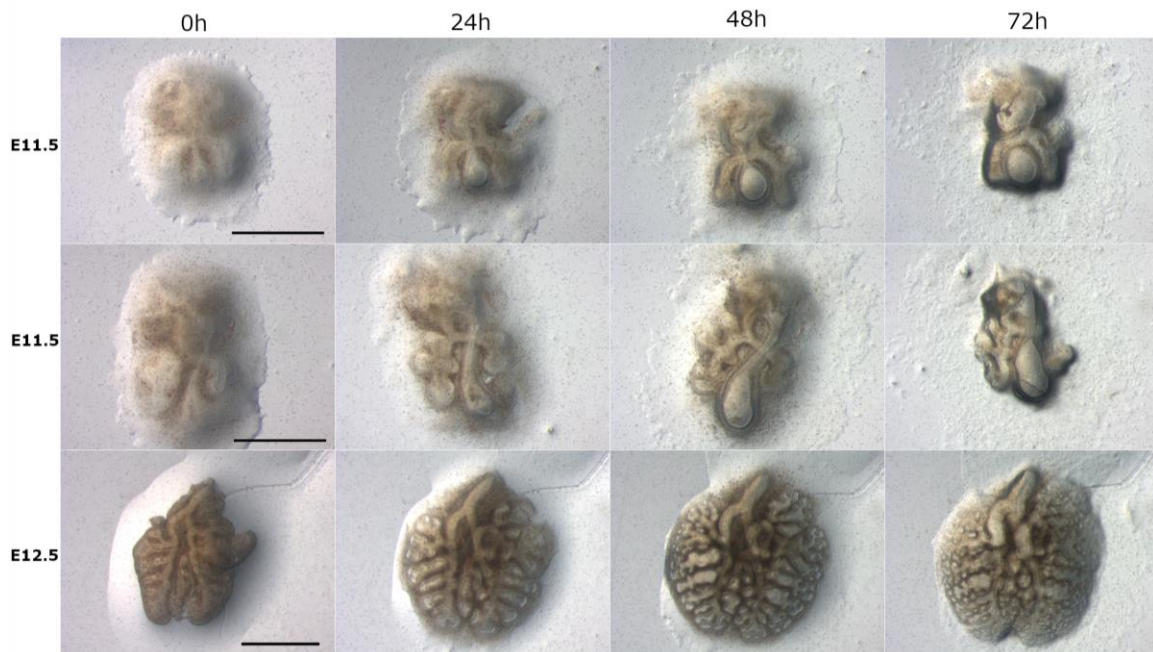


Figure 17. Cultured E11.5 mouse lung explants branched less and had more variability than E12.5 explants.

E11.5 and E12.5 mouse lungs were cultured with PBS (no treatment), 550 $\mu\text{g}/\text{ml}$ of GST or 800 $\mu\text{g}/\text{ml}$ of GST-C-CPE on 8 μm pore filters for 72 hours. Each explant was imaged every 24h. C-CPE-treated explants showed differences in development after 48h of culture compared to controls. Scale bars (1 mm) are displayed in the 0h column and are consistent in each column.

3.3 Treatment with C-CPE decreases the lumen area and the lumen perimeter in embryonic chick lung.

To determine if claudins are important in chick and mouse lungs during the initial stages of branching morphogenesis, lung explants were cultured and treated with the C-CPE reagent that removes specific claudins from tight junctions. E5 chick lungs were dissected and placed into one of three culture conditions: GST-C-CPE in the media, GST control or PBS which acted as a no treatment control (Figure 18). Explanted lungs were photographed every 24 hours and the images were used for morphometric analyses, including measurements of the perimeter of the epithelial airway structures, the lumen area and the bud count. First, I cultured chick lungs with 200 $\mu\text{g}/\text{ml}$ of GST-C-CPE, 100 $\mu\text{g}/\text{ml}$ of GST and PBS. The difference of concentration between GST-C-CPE and

GST is to account for the fact that the molecular weight of GST is 26 kDa while for GST-C-CPE, it is 37 kDa. To standardize the molarity of the two media supplements, the GST was used at a lower concentration than for GST-C-CPE. There were no differences seen between the different groups. Chick lungs treated with 400 $\mu\text{g/ml}$ of GST-C-CPE, 200 $\mu\text{g/ml}$ of GST or PBS did not exhibit differences between treatments. However, chick lungs cultured with 800 $\mu\text{g/ml}$ (Figure 18) had a significant difference in lumen perimeter and lumen area when compared to GST (550 $\mu\text{g/ml}$) and PBS controls after 48 hours of culture (Figure 19 B and C). The change in growth between subsequent timepoints for the lumen perimeter and the lumen area was calculated. There was a significant difference in lumen perimeter growth between GST-C-CPE treated lungs compared to the controls between 0h and the 24h time points and from 24h to the 48h time points. No significance was observed between the 48h and the 72h time points (Figure 19 E). There was a significant difference in the expansion of the lumen area (calculated in folds) between GST-C-CPE treated lungs compared to the controls at every time point (Figure 19 F). The lung bud count was also measured blindly and the average of 3 measurements was used. There were no significant differences between lungs cultured in PBS and lungs cultured in GST (550 $\mu\text{g/ml}$) or in GST-C-CPE (800 $\mu\text{g/ml}$) (Figure 19 D). These data suggest that cultured chick lung explants treated with 800 $\mu\text{g/ml}$ GST-C-CPE did not have an effect on bud number but affected lumen perimeter and lumen area.

3.4 C-CPE localizes to the apical side of the epithelial cells in treated lungs

To confirm that the GST-C-CPE localizes to the apical membrane with the claudins in cultured chick explants, immunofluorescence was performed. CPE antibody, which also recognizes C-CPE, was used on transverse cryosections of chick lungs cultured 12 hours with the addition of 800 $\mu\text{g/ml}$ of GST-C-CPE, 550 $\mu\text{g/ml}$ of GST or PBS. Expression of C-CPE was observed on the apical side of epithelial cells of GST-C-CPE treated lung explants which is where claudins are mainly expressed. No expression was seen on GST or PBS treated explants (Figure 20).

3.5 αSMA immunofluorescence on C-CPE treated chick lung explants was not different than controls

αSMA is important during mammalian lung branching. αSMA appears at basal side of the cells at the tip of a bud right before its bifurcation. When these smooth muscles are surgically removed,

the bud regain its original shape. Also, when α SMA is affected by disrupting FGF signaling or activating SHH signaling, ectopic smooth muscles form and block further branching (Kim *et al.*, 2015). To determine if the phenotype observed in C-CPE treated chick lung explants is due to a change in α SMA expression or localization, explant cryosections were stained with α SMA antibody. α SMA was seen in all groups, but only in a small number of lung buds. It was expressed in the mesenchymal cells at the edge of the basolateral side of the lung epithelial cells. No difference in the orientation, the localization and the quantity of α SMA was observed in the three groups (Figure 21).

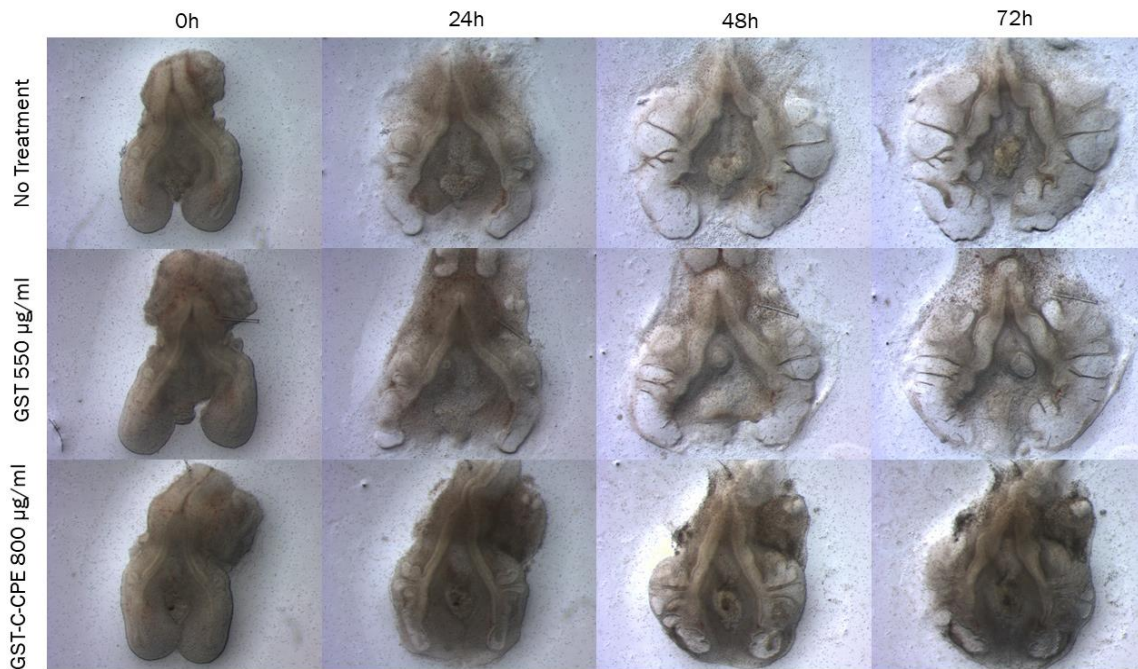


Figure 18. C-CPE affected growth of E5 chick lungs grown in explant culture.

E5 chick lungs were cultured with PBS (no treatment), 550 μ g/ml of GST or 800 μ g/ml of GST-C-CPE on 8 μ m pore filters for 72 hours. Each explant was imaged every 24 hours. C-CPE-treated explants showed differences in development after 48h of culture compared to controls.

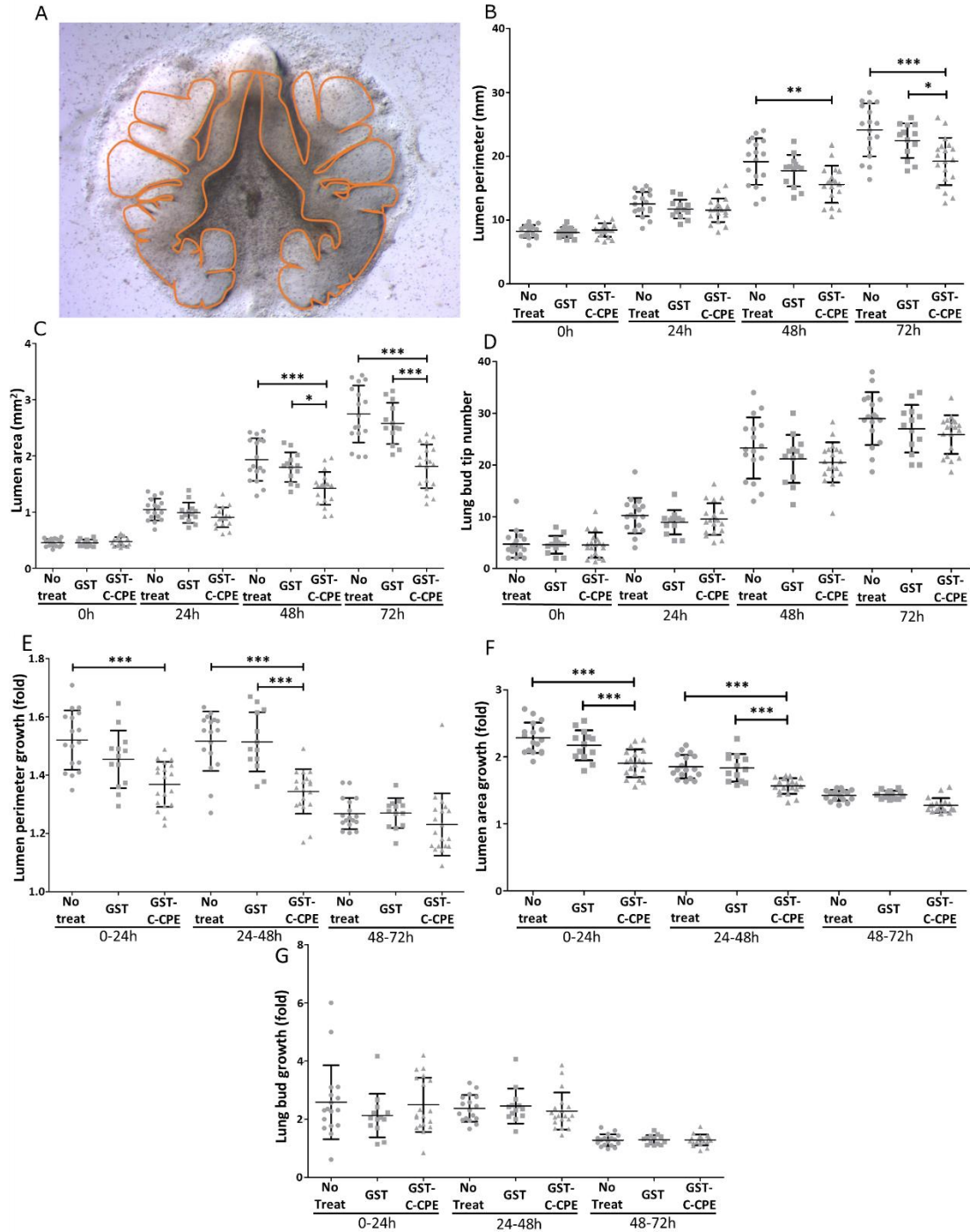


Figure 19. Chick lung explants cultured with 800 µg/ml of C-CPE have a smaller lumen perimeter and lumen area compared to controls.

Measurements of the lumen perimeter (A, B), the lumen area (A, C) and the lung bud number (D) was done every 24h on explants cultured with PBS (no treatment), 550 µg/ml of GST or 800 µg/ml of GST-C-CPE. The lumen perimeter growth (E), the lumen area growth (F) and the lung bud growth (G) was calculated in folds between time points. No treatment : 3 experiments; N=17 | GST : 2 experiments; N=13 | GST-C-CPE : 3 experiments; N=19. Mean (SD); One-way ANOVA with Tukey's Multiple Comparison test, Significance: * : < 0,05 ; ** : < 0,01 ; *** : < 0,001.

3.6 Preliminary results of molecular analysis show partial removal of Claudin-3 in C-CPE treated chick lungs.

To confirm claudin removal from the tight junctions, immunofluorescence targeting Claudin-3, a C-CPE-sensitive claudin, was performed on 10 μm cryosections of chick lungs cultured 12h (Figure 22). In GST and no treatment controls, Claudin-3 was expressed on the apical side of the epithelial cells, colocalizing with ZO-1. In GST-C-CPE treated explants, some Claudin-3 expression is seen in the luminal area and in the cell cytoplasm. This suggests that GST-C-CPE affects Claudin-3 localization in *ex vivo* cultured chick lung explants. However, this was performed on a low number of sections and needs to be repeated to confirm results.

3.7 Treatment with C-CPE seems to decrease lumen area in embryonic mouse lung explants.

E12.5 mouse lungs were cultured in 800 $\mu\text{g}/\text{ml}$ of GST-C-CPE, 550 $\mu\text{g}/\text{ml}$ of GST or PBS (no treatment) (Figure 23). All explants were able to grow and branch similarly. However, the primary and secondary bronchi of the GST-C-CPE treated explants appear smaller than in control explants.

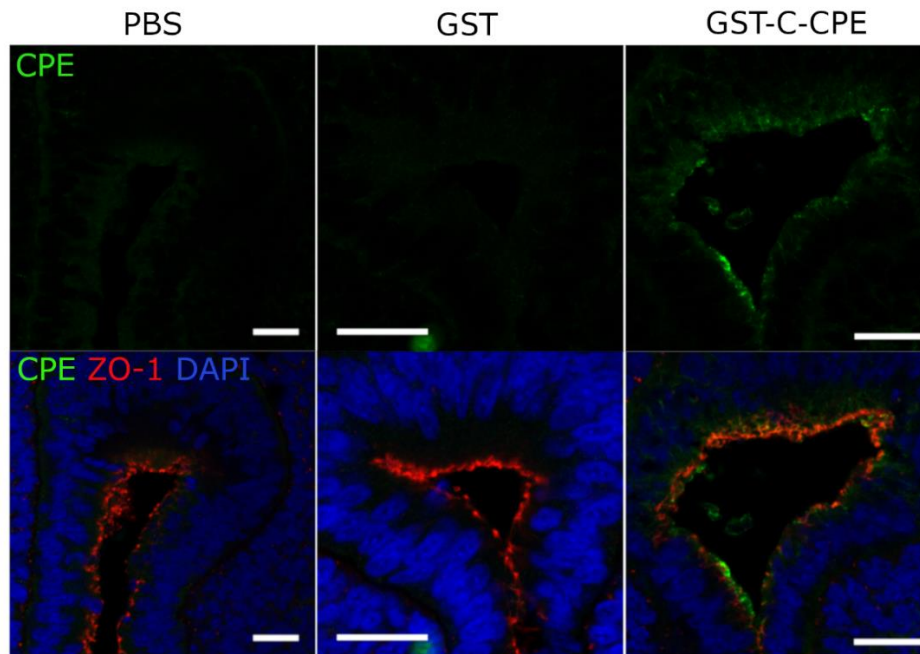


Figure 20. C-CPE localizes to the apical side of epithelial cells in treated lungs

Immunofluorescence targeting CPE (green) and ZO-1 (red) was performed on 10 μm cryosections of chick lung explants previously cultured 12h with PBS (no treatment), 550 $\mu\text{g}/\text{ml}$ of GST or 800 $\mu\text{g}/\text{ml}$ of GST-C-CPE. These sections were imaged using a confocal microscope. Scale bars: 20 μm .

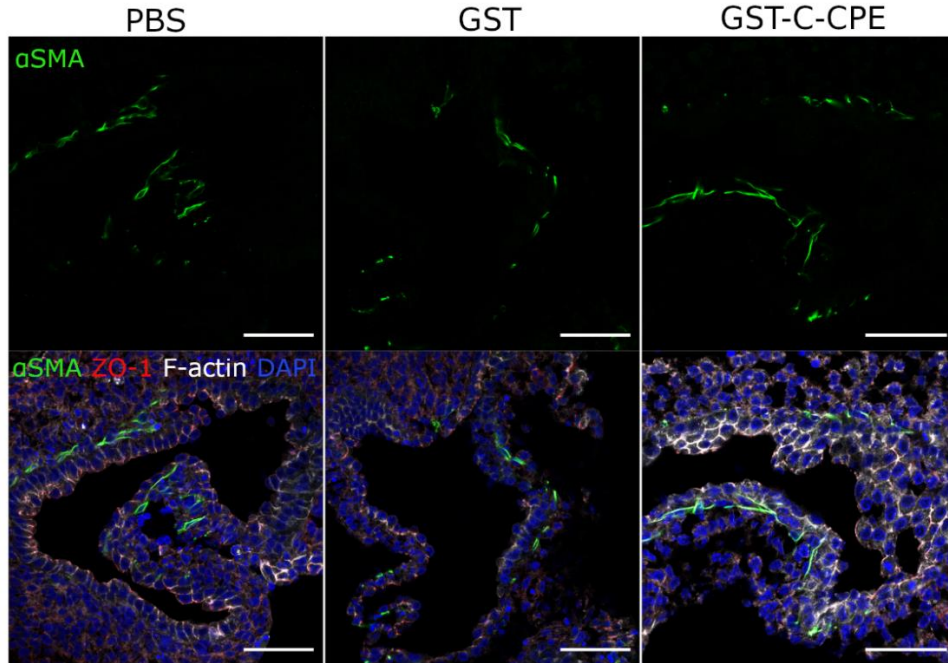


Figure 21. C-CPE treatment did not affect α SMA in chick lung explants.

Immunofluorescence targeting α SMA (green), ZO-1 (red) and F-actin was performed on 10 μ m cryosections of chick lung explants previously cultured 72h with PBS (no treatment), 550 μ g/ml of GST or 800 μ g/ml of GST-C-CPE. These sections were imaged using a confocal microscope. Scale bars: 50 μ m.

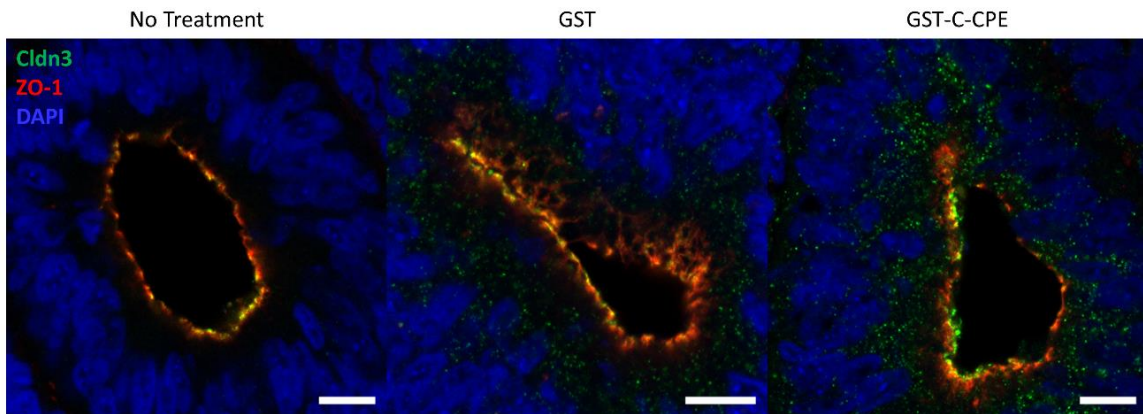


Figure 22. Preliminary results suggest removal of Claudin-3 in C-CPE-treated chick lung explants.

Immunofluorescence targeting Claudin-3 (green) and ZO-1 (red) was performed on 10 μ m cryosections of chick lung explants previously cultured 12 hours with PBS (no treatment), 550 μ g/ml of GST or 800 μ g/ml of GST-C-CPE. These sections were imaged using a confocal microscope. Scale bars: 10 μ m.

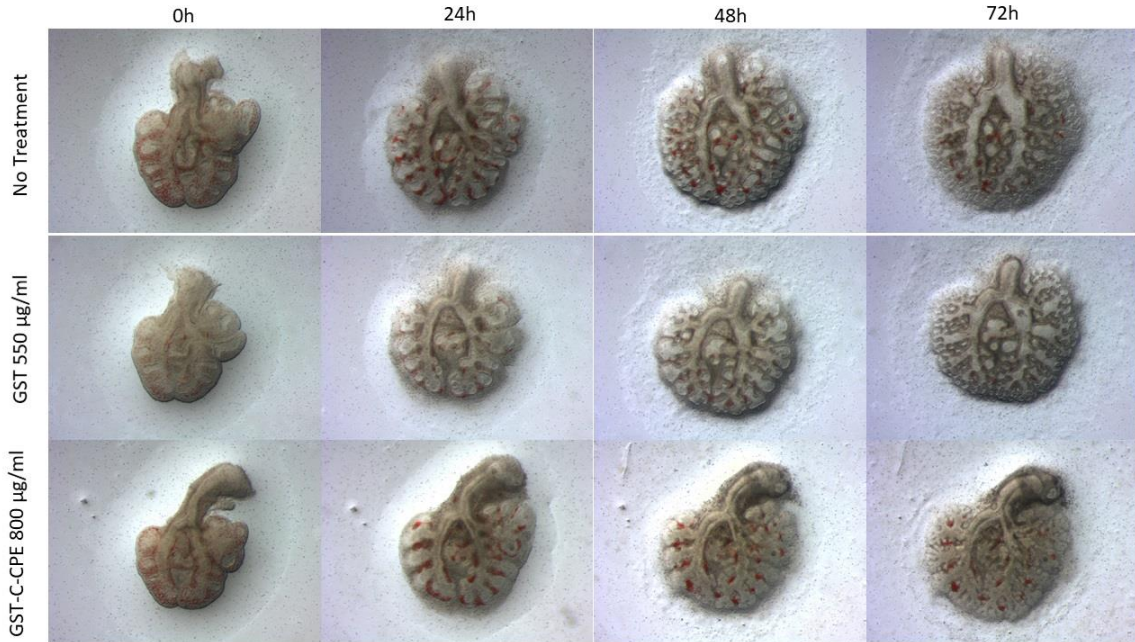


Figure 23. C-CPE treatment did not affect branching in E12.5 mouse lung explants. E12.5 mouse lungs were cultured with PBS (no treatment), 550 µg/ml of GST or 800 µg/ml of GST-C-CPE on 8 µm pore filters for 72 hours. Each explant was imaged every 24h. After 72h of culture, no obvious differences in terminal lung bud number was observed, but the primary and secondary bronchi appear smaller in C-CPE treated explants compared to controls.

3.8 Molecular analysis shows disrupted Claudin-3 localization in GST-C-CPE treated mouse lungs.

To confirm that claudins are really removed from the tight junctions, immunofluorescence targeting Claudin-3, a C-CPE-sensitive claudin, was performed on whole mount mouse lungs cultured 72h (Figure 24). In controls, Claudin-3 was expressed on the apical side of the epithelial cells (Figure 24 A and B). In GST-C-CPE treated explants, Claudin-3 was also expressed on the apical side, but signal was also seen on the basolateral side of the cells (Figure 24 C). This suggests that GST-C-CPE affects Claudin-3 localization in *ex vivo* cultured mouse lung explants. A different concentration of GST was used in figure 24 compared to figure 23 because this experiment was performed before the experiment showed on figure 23. GST has a molecular weight of 26 kDa while GST-C-CPE has a molecular weight of 37 kDa. At a concentration of 400 µg/ml, GST has a molarity of 15.4 µM. At a concentration of 800 µg/ml, GST-C-CPE has a molarity of 21.6 µM. Increasing the concentration of GST to 550 µg/ml brings its molarity to 21.2 µM. This is why, for subsequent experiments, a GST concentration of 550 µg/ml was used.

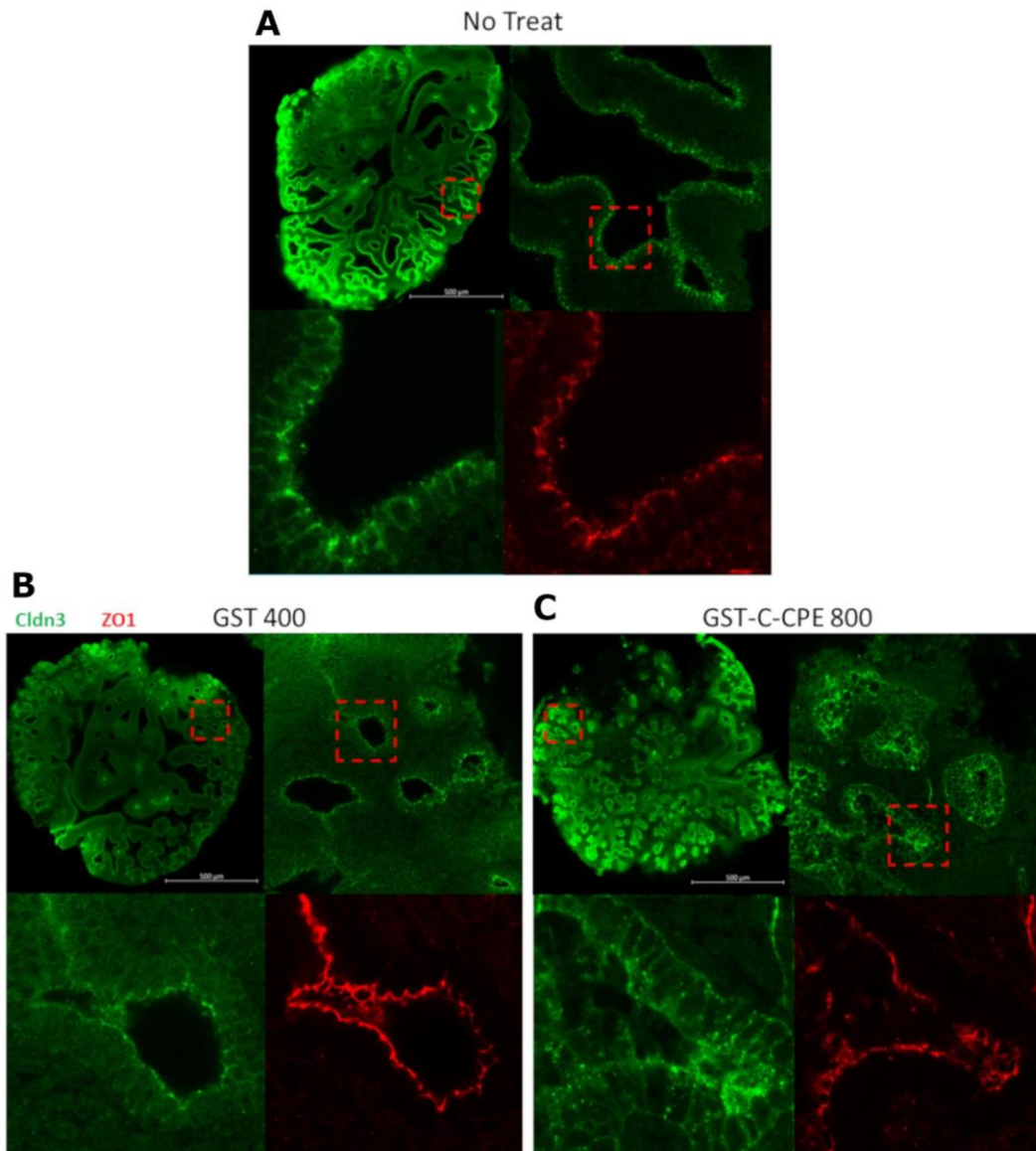


Figure 24. C-CPE treatment affected Claudin-3 localization in cultured mouse lungs. E12.5 mouse lungs were cultured with PBS (no treatment), 400 $\mu\text{g}/\text{ml}$ of GST or 800 $\mu\text{g}/\text{ml}$ of GST-C-CPE on 8 μm pore filters for 72 hours. Immunofluorescence targeting Claudin-3 (green) and ZO-1 (red) was performed on these lungs and imaged using a confocal microscope. C-CPE-treated lungs showed Claudin-3 expression at the apical and the basolateral side of the epithelial cells while controls showed expression only at the apical side of the cells. Scale bars: 500 μm .

CHAPTER 4: Discussion

Lung development starts with the formation of two primary bronchi from the primitive foregut. These two bronchi will then undergo branching morphogenesis when the epithelial cells change shape to form secondary buds. These buds elongate and, in their turn, will bifurcate and form two tubules. These steps occur in repetition for several rounds until the complete three-dimensional structure of the lung is formed. The process of branching morphogenesis is similar between birds and mammals, but it occurs through different mechanisms. In the kidney, which is another branched organ, claudins have been shown to have a role during branching morphogenesis. My project focus was to determine if claudins have similar a role during lung branching morphogenesis. The chick and the mouse embryo were used to determine if the role of claudins is different depending on the species. To determine if claudins are important in lung branching, characterization of claudin expression during the first stages of chick lung branching morphogenesis was performed. Chick and mouse lung explants were also treated with C-CPE to study the effect of the removal of a subset of claudins on lung branching morphogenesis *in vitro*.

4.1 Characterization of claudin expression in chick lung at the formation of secondary bronchi.

Previous studies have looked at claudin expression in the developing lung. In the chick, characterization of the mRNA expression patterns of all claudins was performed on whole embryos at different timepoints during development. *In situ* hybridization on whole embryos may not be sensitive enough to detect low levels of expression within organs. Results for the lung showed *Claudin-1*, *-3* and *-10* mRNA expression in epithelial cells and *Claudin-5* mRNA expression in endothelial cells at different timepoints during lung development (Simard *et al.*, 2005, Collins *et al.*, 2012, Collins *et al.*, 2013). In E12.5 branching mouse lung, immunohistochemistry showed protein expression of Claudin-3, -6 and -7 in epithelial cells and Claudin-5 in endothelial cells. Claudin-1, -2, -4, -8 and -18 protein expression was not observed at this stage and the expression of the remaining claudins was not assessed (Lewis *et al.*, 2018). In my thesis, *in situ* hybridization was performed for a subset of claudins on whole chick lungs at early stages of branching morphogenesis. To determine if the mRNA transcript was translated to a protein and if it was expressed in the tight junctions, protein expression for the same claudin members was characterized by performing immunofluorescence.

My claudin mRNA expression data during the early stages of chick lung branching morphogenesis was generally in agreement with previous results. The claudins that exhibited mRNA expression in epithelial cells, also showed protein expression in epithelial cells at these stages. However, while no mRNA expression was observed for some of the claudins, their protein was detected by immunofluorescence.

The mRNA and protein expression for Claudin-1, -3, -8 and -10 generally correlated in E4, E5 and E6 chick lungs. This is in agreement with previous results which showed *Claudin-1* mRNA expression in epithelial cells of E3, E5 and E8 chick lungs (Simard *et al.*, 2005) and *Claudin-3* mRNA expression in E5, E7 and E10 chick lung epithelial cells (Collins *et al.*, 2013). However, previous results showed *Claudin-10* mRNA expression in E7 and E10 chick lung epithelial cells, but not in E5 chick lungs (Collins *et al.*, 2013). This difference might be due to the fact that I performed *in situ* hybridization on dissected lungs, which is more sensitive than doing it on whole embryos. Claudin-1 and -10 proteins showed higher expression intensity in the primary bronchi compared to the secondary bronchi. This is in contradiction to the mRNA expression data where all epithelial cells expressed *Claudin-1* and -10 mRNA. This suggests that there may be a difference in Claudin-1 and -10 protein expression between the primary bronchi and the secondary bronchi buds. This difference may be independent of mRNA. This might be because the tight junctions in secondary bronchi are not completely established implying that some claudins might be less expressed in immature tight junctions (secondary buds) than in mature tight junctions (primary bronchi).

Claudin-5 expression was surprising because its mRNA and protein was expressed in the endothelial cells of E4 and E5 chick lungs, but protein expression was also seen at the apical side of the epithelial cells in E4, E5 and E6 chick lungs. In past results, *Claudin-5* mRNA was expressed in the vasculature surrounding the lung buds at E4.5, E7 and E9 (Collins *et al.*, 2012). This agrees with the mRNA expression data, but not with the protein expression data. Considering that mRNA detection is more specific than protein detection and that some claudin antibodies have been shown to cross react with other claudins (Suzuki *et al.*, 2009), I believe that Claudin-5 is expressed in endothelial cells of E4, E5 and E6 chick lungs but not in epithelial cells.

Claudin-4 and -14 expression showed differences between mRNA expression and protein expression. In previous results, *Claudin-4* and -14 mRNA were not observed in E5, E7 and E10 chick lung (Collins *et al.*, 2013) agreeing with the present mRNA results. Therefore, I believe that Claudin-4 and Claudin-14 proteins are not expressed in the E4, E5 and E6 chick lungs.

Different reasons might explain these discrepancies between mRNA and protein expression. One explanation is that the half life of the protein may be longer than the half life of the mRNA. For example, Claudin-2 protein has a half-life of 12 hours while the half-life of Claudin-4 protein is 4 hours (Van Itallie *et al.*, 2004). For the mRNA half-life, it can be up to 30 hours depending on the claudin and the factors stabilizing the mRNA (Sharma *et al.*, 2013). Another explanation which might explain the presence of protein, but no mRNA would be that the mRNA is quickly degraded. Different mechanisms might be responsible for this like microRNA-mediated mRNA decay or the binding of long non-coding RNA to the mRNA transcript which would inhibit binding of the antisense probe during *in situ* hybridization. Finally, another reason to explain this difference would be that there is a significant amount of false positive signal from the antibodies in the detection of mRNA or protein.

My expression experiments have shown that Claudin-3 is the only C-CPE-sensitive claudin expressed in epithelial cells during the first stages of chick lung branching morphogenesis. Other claudins that are not specifically targeted by C-CPE might still be affected by treatment with C-CPE through secondary effects. For example, Claudin-1 and -3 are known to interact together in *trans*- (Furuse *et al.*, 1999) therefore, the removal of Claudin-3 by C-CPE may lead to the removal of Claudin-1 as well.

4.2 C-CPE-treated lung explants have reduction in lumen area.

To study the role of claudins in the first stages of lung branching morphogenesis, I cultured chick and mouse embryonic lungs and treated them with C-CPE. C-CPE is a protein which binds to the second extracellular loop of a subset of claudins and remove them from the tight junction. A similar experiment done with embryonic mouse kidney resulted in the reduction of branching morphogenesis. Because at least one C-CPE-sensitive claudin is expressed in the chick and the mouse lung at the early stages of lung branching morphogenesis, I expected that when lung explants are treated with C-CPE, branching morphogenesis would be inhibited.

When chick lung explants were treated with 200, 400 and 600 µg/ml of C-CPE, no differences were observed between treated lungs and controls. However, differences were observed at a treatment of 800 µg/ml of C-CPE. This suggests that a concentration of 600 µg/ml and below does

not affect claudins to the point of creating a phenotype in the cultured lungs. This might be due to the fact that C-CPE is not in direct contact with the lumen of lung bronchi, where it can affect the claudins. It is added to the media and thus only a fraction of the C-CPE may actually end up in the lumen. My results did not show a difference in lung bud counts in chick lung explants treated with 800 µg/ml of C-CPE. This suggests that at least Claudin-3 does not have a direct role in chick lung branching morphogenesis.

Measurements of the lumen perimeter and the lumen area showed a reduction in C-CPE-treated explants compared to controls after 48 hours of culture. This difference in lumen area suggests that C-CPE affects a mechanism controlling the expansion of chick lung lumen. Previous papers showed a role of claudins in regulating turgidity in other luminal structures. For example, C-CPE treatment caused the removal of Claudin-4 and Claudin-6 from the tight junction of developing mouse blastocyst and resulted in a defect in blastocoel expansion. The authors suggested a role of claudins in the formation or the maintenance of the hydrostatic pressure that provides turgidity to the blastocyst (Moriwaki *et al.*, 2007). Also, the loss of Claudin-5a reduces the ventricular lumen volume in the zebrafish embryonic brain. Claudin-5a has a role in sealing the tight junctions to maintain ventricular fluid pressure (Zhang *et al.*, 2010). Similarly, Claudin-15 has a role in facilitating luminal fluid accumulation in the zebrafish gut. However, in contrast to Claudin-5a, Claudin-15 forms an ionic pore which lets Na⁺ and K⁺ pass through the paracellular space from the basolateral to the apical side of the epithelial cells (Bagnat *et al.*, 2007). These experiments suggest that the difference in lumen area observed in C-CPE-treated chick and mouse lung explants could be a consequence of claudin removal.

Immunofluorescence experiments were performed on cultured chick lung explants to determine if C-CPE removes C-CPE-sensitive claudins from the tight junctions. Immunofluorescence assays showed partial removal of Claudin-3. However, the sample size should be increased prior to making any conclusions. Even if Claudin-3 removal is not observed by immunofluorescence, it does not signify that C-CPE does not affect claudins. Only a fraction of Claudin-3 might be removed by C-CPE which might not be visible by immunofluorescence because the assay does not provide enough resolution. This effect might still have consequences on tight junction function and permeability.

In mouse lung experiments, a phenotype similar to the one seen in the chick was observed. There was no observed difference in the branching pattern between mouse lung explants cultured in

GST media and those cultured in C-CPE, although detailed measurements were not performed. Primary and secondary bronchi appeared to have a smaller area in explants treated with C-CPE compared to GST controls. These data show that C-CPE has a similar effect in cultured chick and mouse lung explants.

Claudin-3 immunofluorescence performed on cultured mouse lung explants showed a difference in Claudin-3 localization in C-CPE-treated lungs: expression was seen at the apical and the basolateral side. Immunofluorescence of a non-C-CPE-sensitive claudin still needs to be performed to conclude that this effect is specific to C-CPE-sensitive claudins. This phenotype is different than what is seen in other organs or cell lines treated with C-CPE. In the chick neural tube, treatment with C-CPE causes internalization of C-CPE-sensitive claudins leading to a reduction in their colocalization with ZO-1, a tight junction marker (Baumholtz *et al.*, 2017). This difference in phenotype might be due to the fact that immunofluorescence analysis of C-CPE-treated chick neural tubes was performed after 5 hours of treatment, while I looked later, after 72 hours of culture. This time difference might affect how the tissue responds to the loss of claudins. The cells might be trying to compensate for the loss of claudins at the tight junction by producing more claudin proteins when later time points are examined. For unknown reasons, the excess in claudin proteins was found at the basal side of the cells. Another hypothesis would be that in normal conditions, the claudins are transported to the apical side of the cells to the tight junctions. In a C-CPE environment, the C-CPE-sensitive claudins would be removed from the tight junctions and would circulate freely in the cytoplasm. After a certain amount of time, these proteins would reintegrate into the membrane, but because they are not actively transported to the apical side, they might reintegrate into the membrane at the basolateral side of the cells. Thus, immunofluorescence analysis of C-CPE-sensitive claudins needs to be performed at earlier time points to determine if a claudin removal phenotype similar to the one seen in other C-CPE-treated tissues is observed in mouse lungs. Nonetheless, the observed difference in Claudin-3 localization in C-CPE-treated mouse lung explants suggests that the detected difference in lumen area is due to the alteration of tight junctions through claudin mislocalization by C-CPE.

Published papers have shown that claudins can have a role in regulating lumen fluid accumulation by sealing the paracellular pathway (Zhang *et al.*, 2010) or by creating ionic pores in the tight junction (Bagnat *et al.*, 2007). In the lung, high levels of Cl⁻ ions in the epithelial cells leads to the passive secretion of Cl⁻ ions into the lumen. This creates a negative lumen transepithelial potential

difference which drives the passive transport of Na⁺ inside the tubule. A strong osmotic gradient is formed inside the lumen resulting in the accumulation of lung fluid (Olver *et al.*, 2004). Like in the ventricle of the zebrafish brain, claudins might have a role in sealing the paracellular pathway in the lung epithelial cells. Claudin-3, the only C-CPE-sensitive claudin expressed in branching chick lung, is known to be a sealing claudin (Milatz *et al.*, 2010). This suggests that Claudin-3 in the chick lung could act like Claudin-5a in the zebrafish brain ventricle, sealing the paracellular pathway from the passage of ions from the luminal space. The alteration of Claudin-3 localization by C-CPE would allow the passage of ions in the paracellular pathway from the lumen to the interstitium of the lung, leading to a decrease in osmotic differential in the lumen. This would reduce fluid accumulation in the lumen as seen in C-CPE-treated chick lung explants. In the mouse, C-CPE-sensitive Claudin-3, -6 and -7 are expressed in the lung epithelial cells during branching morphogenesis (Lewis *et al.*, 2018). Claudin-6 is known as a sealing claudin (Sas *et al.*, 2008). Claudin-7's function is controversial: some results suggest Claudin-7 forms anion pores (Hou *et al.*, 2006), while other results suggest it acts as an anion barrier (Alexandre *et al.*, 2005). Nonetheless, two out of the three C-CPE-sensitive claudins that are expressed in the mouse lung during branching morphogenesis are known to be sealing claudins which suggests that these claudins regulate luminal fluid accumulation by blocking ions from passing through the paracellular pathway. However, the removal of Claudin-6 and -7 needs to be assessed in C-CPE-treated mouse lung explants to determine if they are also responsible for the phenotype seen in C-CPE-treated mouse lungs.

To test if claudins have a role in regulating transport in the paracellular pathway in chick and mouse lungs, experiments using small molecules can be performed on cultured lungs. In the zebrafish brain ventricle, injection of lanthanum nitrate, an electron-dense small molecule was injected into the lumen. This is a good way to study tight junction permeability. However, this molecule needs to be used with electron microscopy (Zhang *et al.*, 2010). In the zebrafish gut, two tracers were injected into the yolk to see if they would reach the apical side of the gut epithelial cells. Rhodamine-dextran of relative molecular mass 10,000 and a biotinylation reagent of relative molecular mass 443 were used (Bagnat *et al.*, 2007). This could be used in mouse and chick lung explants to determine if molecules of different size can pass through the tight junction of C-CPE-treated explants. However, this would not determine if the paracellular pathway is more or less permeable to certain ions. To determine this, transepithelial electrical resistance should be used. Unfortunately, transepithelial electrical resistance cannot be used on lung explants as it needs a

single cell layer covering the entire surface of an insert. Performing transepithelial electrical resistance on an epithelial mouse lung cell line like MLE 12 (ATCC® CRL-2110™) might be a good way to test paracellular permeability in lung cells treated with C-CPE.

My results did not show a direct role for C-CPE-sensitive claudins on chick and mouse lung branching morphogenesis. However, they do suggest roles for these claudins in regulating lung luminal fluid accumulation. This role in maintaining turgidity in mouse lung lumen might still have an indirect effect on branching morphogenesis. In fact, internal pressure has been shown to be important during lung branching. Cauterizing the trachea of embryonic mouse lung explants, which increases internal pressure, promotes branching morphogenesis through the Fgf10/Fgfr2b/Sprouty2 pathway (Unbekandt *et al.*, 2008). Drainage of the luminal fluid has also been shown to decrease lung growth and development in embryonic sheep lung (Moessinger *et al.*, 1990). Also, C-CPE only targets a subset of claudins. Therefore, other claudins might still have a more direct role in lung branching morphogenesis. More experiments need to be done to target other claudins and to study their role during lung branching morphogenesis.

CHAPTER 5: Conclusions and future directions

In my thesis project, I showed that the mRNA and the protein of Claudin-1, -3 and -10 are expressed in the epithelial cells of chick lungs at E4, E5 and E6. Protein expression showed that they colocalize with ZO-1, suggesting that they are localized at the tight junction. Other claudin proteins were detected, but mRNA expression was not in agreement with these results, thus further experiments are needed to confirm these expression patterns.

To test whether claudins are important during the first stages of chick and mouse lung branching morphogenesis, lung explants were cultured with C-CPE, a protein which removes a subset of claudins from the tight junction. In chick lung and mouse explant culture, C-CPE treatment did not affect the total number of terminal buds. However, in chick lung explants, C-CPE-treated samples exhibited a significant decrease in perimeter and lumen area after 48 hours of culture. A similar phenotype was observed in mouse lung culture explants, but further measurements are needed to confirm the findings in the mouse.

To determine if C-CPE-sensitive claudins were actually removed from the tight junctions, Claudin-3 immunofluorescence was performed on chick lung explant sections and on whole mount mouse lung explants. Chick lung explants cultured 12 and 72 hours showed a partial decrease in luminal staining suggesting partial removal of Claudin-3, but more experiments are needed to confirm these findings and show significance. In whole mouse lung explants cultured for 72 hours, basolateral expression of Claudin-3 was observed in C-CPE treated explants while GST control explants showed expression only at the apical side of the epithelial cells. These preliminary data suggest that claudin localization is affected by the presence of C-CPE.

Together, the results suggest that the alteration of the claudin complex by C-CPE does not result in a branching defect in chick or in mouse lungs. However, a reduction in lumen area in the chick and the mouse suggests a role for C-CPE-sensitive claudins in regulating lumen fluid accumulation in the lung. To confirm this hypothesis, experiments using small molecules should be performed to determine if alteration of tight junctions by C-CPE affects the paracellular pathway. However, these assays cannot indicate if the ionic permeability is affected. To examine this aspect, transepithelial electric resistance could be used. However, it can only be performed on a single cell layer. A mouse lung epithelial cell line could be used to assess permeability differences in C-CPE-treated samples.

It is still possible that other claudins are involved in the lung branching morphogenesis process and targeting non-C-CPE-sensitive claudins could lead to lung branching defects. However, my results suggest a role of the C-CPE-sensitive claudins in regulating luminal fluid accumulation in chick and mouse lung during branching morphogenesis. This role could be important to maintain the turgidity of the lung tubules during development.

CHAPTER 6: References

- Affolter, M., R. Zeller and E. Caussinus (2009). Tissue remodelling through branching morphogenesis. Nature reviews molecular cell biology **10**(12): 831-842.
- Alexandre, M. D., Q. Lu and Y.-H. Chen (2005). Overexpression of claudin-7 decreases the paracellular Cl⁻ conductance and increases the paracellular Na⁺ conductance in LLC-PK1 cells. Journal of cell science **118**(12): 2683-2693.
- Anderson, W. J., Q. Zhou, V. Alcalde, O. F. Kaneko, L. J. Blank, R. I. Sherwood, J. S. Guseh, J. Rajagopal and D. A. Melton (2008). Genetic targeting of the endoderm with claudin-6CreER. Developmental dynamics **237**(2): 504-512.
- Bagnat, M., I. D. Cheung, K. E. Mostov and D. Y. Stainier (2007). Genetic control of single lumen formation in the zebrafish gut. Nature cell biology **9**(8): 954-960.
- Balda, M. S., J. A. Whitney, C. Flores, S. González, M. Cereijido and K. Matter (1996). Functional dissociation of paracellular permeability and transepithelial electrical resistance and disruption of the apical-basolateral intramembrane diffusion barrier by expression of a mutant tight junction membrane protein. The Journal of cell biology **134**(4): 1031-1049.
- Balda, M. S., C. Flores-Maldonado, M. Cereijido and K. Matter (2000). Multiple domains of occludin are involved in the regulation of paracellular permeability. Journal of cellular biochemistry **78**(1): 85-96.
- Baumholtz, A. I., A. Simard, E. Nikolopoulou, M. Oosenbrug, M. M. Collins, A. Piontek, G. Krause, J. Piontek, N. D. Greene and A. K. Ryan (2017). Claudins are essential for cell shape changes and convergent extension movements during neural tube closure. Developmental biology **428**(1): 25-38.
- Bazzoni, G., O. M. Martínez-Estrada, F. Orsenigo, M. Cordenonsi, S. Citi and E. Dejana (2000). Interaction of junctional adhesion molecule with the tight junction components ZO-1, cingulin, and occludin. Journal of biological chemistry **275**(27): 20520-20526.
- Ben-Yosef, T., I. A. Belyantseva, T. L. Saunders, E. D. Hughes, K. Kawamoto, C. M. Van Itallie, L. A. Beyer, K. Halsey, D. J. Gardner and E. R. Wilcox (2003). Claudin 14 knockout mice, a model for autosomal recessive deafness DFNB29, are deaf due to cochlear hair cell degeneration. Human molecular genetics **12**(16): 2049-2061.
- Bronstein, J., P. Micevych and K. Chen (1997). Oligodendrocyte-specific protein (OSP) is a major component of CNS myelin. Journal of neuroscience research **50**(5): 713-720.
- Colegio, O. R., C. M. Van Itallie, H. J. McCrea, C. Rahner and J. M. Anderson (2002). Claudins create charge-selective channels in the paracellular pathway between epithelial cells. American journal of physiology-cell physiology **283**(1): C142-C147.
- Collins, M. M., A. I. Baumholtz and A. K. Ryan (2012). Claudin-5 expression in the vasculature of the developing chick embryo. Gene expression patterns **12**(3): 123-129.

- Collins, M. M., A. I. Baumholtz and A. K. Ryan (2013). Claudin family members exhibit unique temporal and spatial expression boundaries in the chick embryo. Tissue barriers **1**(3): e24517.
- Collins, M. M., A. I. Baumholtz, A. Simard, M. Gregory, D. G. Cyr and A. K. Ryan (2015). Claudin-10 is required for relay of left–right patterning cues from Hensen’s node to the lateral plate mesoderm. Developmental biology **401**(2): 236-248.
- Cording, J., J. Berg, N. Käding, C. Bellmann, C. Tscheik, J. K. Westphal, S. Milatz, D. Günzel, H. Wolburg and J. Piontek (2012). Tight junctions: Claudins regulate the interactions between occludin, tricellulin and marvelD3, which, inversely, modulate claudin oligomerization. Journal of cell science: jcs. 114306.
- Daugherty, B. L., M. Mateescu, A. S. Patel, K. Wade, S. Kimura, L. W. Gonzales, S. Guttentag, P. L. Ballard and M. Koval (2004). Developmental regulation of claudin localization by fetal alveolar epithelial cells. American journal of physiology-lung cellular and molecular physiology **287**(6): L1266-L1273.
- Daugherty, B. L., C. Ward, T. Smith, J. D. Ritzenthaler and M. Koval (2007). Regulation of heterotypic claudin compatibility. Journal of biological chemistry **282**(41): 30005-30013.
- Ding, L., Z. Lu, O. Foreman, R. Tatum, Q. Lu, R. Renegar, J. Cao and Y. H. Chen (2012). Inflammation and disruption of the mucosal architecture in claudin-7–deficient mice. Gastroenterology **142**(2): 305-315.
- Ebnet, K., C. U. Schulz, M.-K. M. zu Brickwedde, G. G. Pendl and D. Vestweber (2000). Junctional adhesion molecule interacts with the PDZ domain-containing proteins AF-6 and ZO-1. Journal of biological chemistry **275**(36): 27979-27988.
- Ebnet, K., A. Suzuki, S. Ohno and D. Vestweber (2004). Junctional adhesion molecules (JAMs): more molecules with dual functions? Journal of cell science **117**(1): 19-29.
- Fanning, A. S., B. J. Jameson, L. A. Jesaitis and J. M. Anderson (1998). The tight junction protein ZO-1 establishes a link between the transmembrane protein occludin and the actin cytoskeleton. Journal of biological chemistry **273**(45): 29745-29753.
- Farquhar, M. G. and G. E. Palade (1963). Junctional complexes in various epithelia. The Journal of cell biology **17**(2): 375-412.
- Fujita, K., J. Katahira, Y. Horiguchi, N. Sonoda, M. Furuse and S. Tsukita (2000). Clostridium perfringens enterotoxin binds to the second extracellular loop of claudin-3, a tight junction integral membrane protein. FEBS letters **476**(3): 258-261.
- Furuse, M., T. Hirase, M. Itoh, A. Nagafuchi, S. Yonemura and S. Tsukita (1993). Occludin: a novel integral membrane protein localizing at tight junctions. The Journal of cell biology **123**(6): 1777-1788.
- Furuse, M., M. Itoh, T. Hirase, A. Nagafuchi, S. Yonemura and S. Tsukita (1994). Direct association of occludin with ZO-1 and its possible involvement in the localization of occludin at tight junctions. The Journal of cell biology **127**(6): 1617-1626.

Furuse, M., K. Fujita, T. Hiiragi, K. Fujimoto and S. Tsukita (1998). Claudin-1 and-2: novel integral membrane proteins localizing at tight junctions with no sequence similarity to occludin. The Journal of cell biology **141**(7): 1539-1550.

Furuse, M., H. Sasaki and S. Tsukita (1999). Manner of interaction of heterogeneous claudin species within and between tight junction strands. The Journal of cell biology **147**(4): 891-903.

Furuse, M., M. Hata, K. Furuse, Y. Yoshida, A. Haratake, Y. Sugitani, T. Noda, A. Kubo and S. Tsukita (2002). Claudin-based tight junctions are crucial for the mammalian epidermal barrier: a lesson from claudin-1-deficient mice. The Journal of cell biology **156**(6): 1099-1111.

Gamero-Estevez, E., A. Baumholtz and A. K. Ryan (2018). Developing a link between toxicants, claudins and neural tube defects. Reproductive toxicology **81**(1): 155-167.

Gow, A., C. M. Southwood, J. S. Li, M. Pariali, G. P. Riordan, S. E. Brodie, J. Danias, J. M. Bronstein, B. Kachar and R. A. Lazzarini (1999). CNS myelin and sertoli cell tight junction strands are absent in Osp/claudin-11 null mice. Cell **99**(6): 649-659.

Gow, A., C. Davies, C. M. Southwood, G. Frolenkov, M. Chrustowski, L. Ng, D. Yamauchi, D. C. Marcus and B. Kachar (2004). Deafness in Claudin 11-null mice reveals the critical contribution of basal cell tight junctions to stria vascularis function. Journal of neuroscience **24**(32): 7051-7062.

Gupta, I. and A. Ryan (2010). Claudins: unlocking the code to tight junction function during embryogenesis and in disease. Clinical genetics **77**(4): 314-325.

Haddad, N., J. El Andaloussi, H. Khairallah, M. Yu, A. K. Ryan and I. R. Gupta (2011). The tight junction protein claudin-3 shows conserved expression in the nephric duct and ureteric bud and promotes tubulogenesis in vitro. American journal of physiology-renal physiology **301**(5): F1057-F1065.

Hamazaki, Y., M. Itoh, H. Sasaki, M. Furuse and S. Tsukita (2002). Multi-PDZ domain protein 1 (MUPP1) is concentrated at tight junctions through its possible interaction with claudin-1 and junctional adhesion molecule. Journal of biological chemistry **277**(1): 455-461.

Hashizume, A., T. Ueno, M. Furuse, S. Tsukita, Y. Nakanishi and Y. Hieda (2004). Expression patterns of claudin family of tight junction membrane proteins in developing mouse submandibular gland. Developmental dynamics **231**(2): 425-431.

Haskins, J., L. Gu, E. S. Wittchen, J. Hibbard and B. R. Stevenson (1998). ZO-3, a novel member of the MAGUK protein family found at the tight junction, interacts with ZO-1 and occludin. The Journal of cell biology **141**(1): 199-208.

Hou, J., A. S. Gomes, D. L. Paul and D. A. Goodenough (2006). Study of claudin function by RNA interference. Journal of biological chemistry **281**(47): 36117-36123.

Hou, J., Q. Shan, T. Wang, A. S. Gomes, Q. Yan, D. L. Paul, M. Bleich and D. A. Goodenough (2007). Transgenic RNAi depletion of claudin-16 and the renal handling of magnesium. Journal of biological chemistry **282**(23): 17114-17122.

- Hou, J., A. Renigunta, J. Yang and S. Waldegger (2010). Claudin-4 forms paracellular chloride channel in the kidney and requires claudin-8 for tight junction localization. Proceedings of the national academy of sciences **107**(42): 18010-18015.
- Hou, J., M. Rajagopal and A. S. Yu (2013). Claudins and the kidney. Annual review of physiology **75**: 479-501.
- Itoh, M., M. Furuse, K. Morita, K. Kubota, M. Saitou and S. Tsukita (1999). Direct binding of three tight junction-associated MAGUKs, ZO-1, ZO-2, and ZO-3, with the COOH termini of claudins. The Journal of cell biology **147**(6): 1351-1363.
- Itoh, M., H. Sasaki, M. Furuse, H. Ozaki, T. Kita and S. Tsukita (2001). Junctional adhesion molecule (JAM) binds to PAR-3: a possible mechanism for the recruitment of PAR-3 to tight junctions. The Journal of cell biology **154**(3): 491-498.
- Jimenez, F. R., S. T. Belgique, J. B. Lewis, S. A. Albright, C. M. Jones, B. M. Howell, A. P. Mika, T. R. Jergensen, J. R. Gassman and R. J. Morris (2016). Conditional pulmonary over-expression of Claudin 6 during embryogenesis delays lung morphogenesis. International journal of developmental biology **59**(10-11-12): 479-485.
- Kaarteenaho, R., H. Merikallio, S. Lehtonen, T. Harju and Y. Soini (2010). Divergent expression of claudin-1,-3,-4,-5 and-7 in developing human lung. Respiratory research **11**(1): 1-10.
- Kage, H., P. Flodby, D. Gao, Y. H. Kim, C. N. Marconett, L. DeMaio, K.-J. Kim, E. D. Crandall and Z. Borok (2014). Claudin 4 knockout mice: normal physiological phenotype with increased susceptibility to lung injury. American journal of physiology-lung cellular and molecular physiology **307**(7): L524-L536.
- Katahira, J., H. Sugiyama, N. Inoue, Y. Horiguchi, M. Matsuda and N. Sugimoto (1997). Clostridium perfringens enterotoxin utilizes two structurally related membrane proteins as functional receptors in vivo. Journal of biological chemistry **272**(42): 26652-26658.
- Kerr, J., J. El Andaloussi, Y. Yamanaka, A. Ryan and I. Gupta (2015). Claudin 3 CRISPR Knockout Mice are Healthy and Fertile. The FASEB journal **29**(1 Supplement): 666.613.
- Khairallah, H. (2013). Claudins Are Required for Ureteric Bud Branching in the Mouse Embryonic Kidney., McGill University.
- Kim, H. Y., V. D. Varner and C. M. Nelson (2013). Apical constriction initiates new bud formation during monopodial branching of the embryonic chicken lung. Development **140**(15): 3146-3155.
- Kim, H. Y., M.-F. Pang, V. D. Varner, L. Kojima, E. Miller, D. C. Radisky and C. M. Nelson (2015). Localized smooth muscle differentiation is essential for epithelial bifurcation during branching morphogenesis of the mammalian lung. Developmental cell **34**(6): 719-726.
- Kitajiri, S.-i., T. Miyamoto, A. Mineharu, N. Sonoda, K. Furuse, M. Hata, H. Sasaki, Y. Mori, T. Kubota and J. Ito (2004). Compartmentalization established by claudin-11-based tight junctions in stria vascularis is required for hearing through generation of endocochlear potential. Journal of cell science **117**(21): 5087-5096.

Krause, G., L. Winkler, S. L. Mueller, R. F. Haseloff, J. Piontek and I. E. Blasig (2008). Structure and function of claudins. Biochimica et biophysica acta **1778**(3): 631-645.

Kubota, K., M. Furuse, H. Sasaki, N. Sonoda, K. Fujita, A. Nagafuchi and S. Tsukita (1999). Ca²⁺-independent cell-adhesion activity of claudins, a family of integral membrane proteins localized at tight junctions. Current biology **9**(18): 1035-S1031.

LaFemina, M. J., K. M. Sutherland, T. Bentley, L. W. Gonzales, L. Allen, C. J. Chapin, D. Rokkam, K. A. Sweerus, L. G. Dobbs, P. L. Ballard and J. A. Frank (2014). Claudin-18 deficiency results in alveolar barrier dysfunction and impaired alveologenesis in mice. American journal of respiratory cell and molecular biology **51**(4): 550-558.

Lewis, J. B., F. R. Jimenez, B. J. Merrell, B. Kimbler, J. A. Arroyo and P. R. Reynolds (2018). The expression profile of Claudin family members in the developing mouse lung and expression alterations resulting from exposure to secondhand smoke (SHS). Experimental lung research **44**(1): 13-24.

Li, G., P. Flodby, J. Luo, H. Kage, A. Sipos, D. Gao, Y. Ji, L. L. Beard, C. N. Marconett, L. DeMaio, Y. H. Kim, K. J. Kim, I. A. Laird-Offringa, P. Minoo, J. M. Liebler, B. Zhou, E. D. Crandall and Z. Borok (2014). Knockout mice reveal key roles for claudin 18 in alveolar barrier properties and fluid homeostasis. American journal of respiratory cell and molecular biology **51**(2): 210-222.

Liu, F., M. Koval, S. Ranganathan, S. Fanayan, W. S. Hancock, E. K. Lundberg, R. C. Beavis, L. Lane, P. Duek, L. McQuade, N. L. Kelleher and M. S. Baker (2016). Systems Proteomics View of the Endogenous Human Claudin Protein Family. Journal of proteome research **15**(2): 339-359.

Lourenço, S. V., C. M. Coutinho-Camillo, M. E. Buim, S. H. Uyekita and F. A. Soares (2007). Human salivary gland branching morphogenesis: morphological localization of claudins and its parallel relation with developmental stages revealed by expression of cytoskeleton and secretion markers. Histochemistry and cell biology **128**(4): 361-369.

McCarthy, K. M., I. B. Skare, M. C. Stankewich, M. Furuse, S. Tsukita, R. A. Rogers, R. D. Lynch and E. E. Schneeberger (1996). Occludin is a functional component of the tight junction. Journal of cell science **109**(9): 2287-2298.

McClane, B. A. (2001). The complex interactions between Clostridium perfringens enterotoxin and epithelial tight junctions. Toxicon **39**(11): 1781-1791.

Milatz, S., S. M. Krug, R. Rosenthal, D. Günzel, D. Müller, J.-D. Schulzke, S. Amasheh and M. Fromm (2010). Claudin-3 acts as a sealing component of the tight junction for ions of either charge and uncharged solutes. Biochimica et biophysica acta (BBA)-biomembranes **1798**(11): 2048-2057.

Miyamoto, T., K. Morita, D. Takemoto, K. Takeuchi, Y. Kitano, T. Miyakawa, K. Nakayama, Y. Okamura, H. Sasaki and Y. Miyachi (2005). Tight junctions in Schwann cells of peripheral myelinated axons. Journal of cell biology **169**(3): 527-538.

Moessinger, A., R. Harding, T. Adamson, M. Singh and G. Kiu (1990). Role of lung fluid volume in growth and maturation of the fetal sheep lung. The Journal of clinical investigation **86**(4): 1270-1277.

Morita, K., H. Sasaki, K. Fujimoto, M. Furuse and S. Tsukita (1999). Claudin-11/OSP-based tight junctions of myelin sheaths in brain and Sertoli cells in testis. The Journal of cell biology **145**(3): 579-588.

Moriwaki, K., S. Tsukita and M. Furuse (2007). Tight junctions containing claudin 4 and 6 are essential for blastocyst formation in preimplantation mouse embryos. Developmental biology **312**(2): 509-522.

Moura, R. S., J. P. Coutinho-Borges, A. P. Pacheco, P. O. Damota and J. Correia-Pinto (2011). FGF signaling pathway in the developing chick lung: expression and inhibition studies. PLoS one **6**(3): e17660.

Mruk, D. D. and C. Y. Cheng (2015). The mammalian blood-testis barrier: its biology and regulation. Endocrine reviews **36**(5): 564-591.

Muto, S., M. Hata, J. Taniguchi, S. Tsuruoka, K. Moriwaki, M. Saitou, K. Furuse, H. Sasaki, A. Fujimura and M. Imai (2010). Claudin-2-deficient mice are defective in the leaky and cation-selective paracellular permeability properties of renal proximal tubules. Proceedings of the national academy of sciences **107**(17): 8011-8016.

Nitta, T., M. Hata, S. Gotoh, Y. Seo, H. Sasaki, N. Hashimoto, M. Furuse and S. Tsukita (2003). Size-selective loosening of the blood-brain barrier in claudin-5-deficient mice. The Journal of cell biology **161**(3): 653-660.

Odenwald, M. A., W. Choi, A. Buckley, N. Shashikanth, N. E. Joseph, Y. Wang, M. H. Warren, M. M. Buschmann, R. Pavlyuk and J. Hildebrand (2017). ZO-1 interactions with F-actin and occludin direct epithelial polarization and single lumen specification in 3D culture. Journal of cell science **130**(1): 243-259.

Olver, R. E., D. V. Walters and S. M. Wilson (2004). Developmental regulation of lung liquid transport. Annual review of physiology **66**: 77-101.

Patel, V. N., I. T. Rebustini and M. P. Hoffman (2006). Salivary gland branching morphogenesis. Differentiation **74**(7): 349-364.

Rackley, C. R. and B. R. Stripp (2012). Building and maintaining the epithelium of the lung. The Journal of clinical investigation **122**(8): 2724-2730.

Saitou, M., M. Furuse, H. Sasaki, J.-D. Schulzke, M. Fromm, H. Takano, T. Noda and S. Tsukita (2000). Complex phenotype of mice lacking occludin, a component of tight junction strands. Molecular biology of the cell **11**(12): 4131-4142.

Sas, D., M. Hu, O. W. Moe and M. Baum (2008). Effect of claudins 6 and 9 on paracellular permeability in MDCK II cells. American journal of physiology-regulatory, integrative and comparative physiology **295**(5): R1713-R1719.

- Schlingmann, B., S. A. Molina and M. Koval (2015). Claudins: Gatekeepers of lung epithelial function. Seminars in cell and developmental biology **42**: 47-57.
- Schmidt, A., D. Utepbergenov, S. Mueller, M. Beyermann, J. Schneider-Mergener, G. Krause and I. Blasig (2004). Occludin binds to the SH3-hinge-GuK unit of zonula occludens protein 1: potential mechanism of tight junction regulation. Cellular and molecular life sciences **61**(11): 1354-1365.
- Sharma, A., A. A. Bhat, M. Krishnan, A. B. Singh and P. Dhawan (2013). Trichostatin-A modulates claudin-1 mRNA stability through the modulation of Hu antigen R and tristetraproline in colon cancer cells. Carcinogenesis **34**(11): 2610-2621.
- Simard, A., E. Di Pietro and A. K. Ryan (2005). Gene expression pattern of Claudin-1 during chick embryogenesis. Gene expression patterns **5**(4): 553-560.
- Simard, A., E. Di Pietro, C. R. Young, S. Plaza and A. K. Ryan (2006). Alterations in heart looping induced by overexpression of the tight junction protein Claudin-1 are dependent on its C-terminal cytoplasmic tail. Mechanisms of development **123**(3): 210-227.
- Sonoda, N., M. Furuse, H. Sasaki, S. Yonemura, J. Katahira, Y. Horiguchi and S. Tsukita (1999). Clostridium perfringens Enterotoxin Fragment Removes Specific Claudins from Tight Junction Strands Evidence for Direct Involvement of Claudins in Tight Junction Barrier. The Journal of cell biology **147**(1): 195-204.
- Suzuki, M., M. Kato-Nakano, S. Kawamoto, A. Furuya, Y. Abe, H. Misaka, N. Kimoto, K. Nakamura, S. Ohta and H. Ando (2009). Therapeutic antitumor efficacy of monoclonal antibody against Claudin-4 for pancreatic and ovarian cancers. Cancer science **100**(9): 1623-1630.
- Szaszi, K. and Y. Amoozadeh (2014). New insights into functions, regulation, and pathological roles of tight junctions in kidney tubular epithelium. International review of cell and molecular biology, Elsevier. **308**: 205-271.
- Tamura, A., Y. Kitano, M. Hata, T. Katsuno, K. Moriwaki, H. Sasaki, H. Hayashi, Y. Suzuki, T. Noda and M. Furuse (2008). Megaintestine in claudin-15-deficient mice. Gastroenterology **134**(2): 523-534. e523.
- Tanaka, M., R. Kamata and R. Sakai (2005). EphA2 phosphorylates the cytoplasmic tail of Claudin-4 and mediates paracellular permeability. Journal of biological chemistry **280**(51): 42375-42382.
- Tatum, R., Y. Zhang, K. Salleng, Z. Lu, J.-J. Lin, Q. Lu, B. G. Jeansonne, L. Ding and Y.-H. Chen (2009). Renal salt wasting and chronic dehydration in claudin-7-deficient mice, American Physiological Society Bethesda, MD.
- Umeda, K., T. Matsui, M. Nakayama, K. Furuse, H. Sasaki, M. Furuse and S. Tsukita (2004). Establishment and characterization of cultured epithelial cells lacking expression of ZO-1. Journal of biological chemistry **279**(43): 44785-44794.

- Unbekandt, M., P.-M. del Moral, F. G. Sala, S. Bellusci, D. Warburton and V. Fleury (2008). Tracheal occlusion increases the rate of epithelial branching of embryonic mouse lung via the FGF10-FGFR2b-Sprouty2 pathway. Mechanisms of development **125**(3-4): 314-324.
- Van Itallie, C., C. Rahner and J. M. Anderson (2001). Regulated expression of claudin-4 decreases paracellular conductance through a selective decrease in sodium permeability. The Journal of clinical investigation **107**(10): 1319-1327.
- Van Itallie, C., O. Colegio and J. Anderson (2004). The cytoplasmic tails of claudins can influence tight junction barrier properties through effects on protein stability. The Journal of Membrane Biology **199**(1): 29-38.
- Van Itallie, C. M., T. M. Gambling, J. L. Carson and J. M. Anderson (2005). Palmitoylation of claudins is required for efficient tight-junction localization. Journal of cell science **118**(7): 1427-1436.
- Van Itallie, C. M., L. L. Mitic and J. M. Anderson (2011). Claudin-2 forms homodimers and is a component of a high molecular weight protein complex. Journal of biological chemistry **286**(5): 3442-3450.
- Van Itallie, C. M., A. J. Tietgens, K. LoGrande, A. Aponte, M. Gucek and J. M. Anderson (2012). Phosphorylation of claudin-2 on serine 208 promotes membrane retention and reduces trafficking to lysosomes. Journal of cell science: jcs. 111237.
- Van Itallie, C. M., A. J. Tietgens and J. M. Anderson (2017). Visualizing the dynamic coupling of claudin strands to the actin cytoskeleton through ZO-1. Molecular biology of the cell **28**(4): 524-534.
- Varner, V. D. and C. M. Nelson (2014). Cellular and physical mechanisms of branching morphogenesis. Development **141**(14): 2750-2759.
- Watanabe, T. and F. Costantini (2004). Real-time analysis of ureteric bud branching morphogenesis in vitro. Developmental biology **271**(1): 98-108.
- Wittchen, E. S., J. Haskins and B. R. Stevenson (1999). Protein interactions at the tight junction: actin has multiple binding partners, and ZO-1 forms independent complexes with ZO-2 and ZO-3. Journal of biological chemistry **274**(49): 35179-35185.
- Zhang, J., J. Piontek, H. Wolburg, C. Piehl, M. Liss, C. Otten, A. Christ, T. E. Willnow, I. E. Blasig and S. Abdelilah-Seyfried (2010). Establishment of a neuroepithelial barrier by Claudin5a is essential for zebrafish brain ventricular lumen expansion. Proceedings of the national academy of sciences **107**(4): 1425-1430.